DATE PALM LEAF EXTRACT (DPLE) AS A GREEN CORROSION INHIBITOR FOR COPPER IN RAW WATER

BY

ABDUL-RAHMAN A. H. NOUR

A Thesis Presented to the
DEANSHIP OF GRADUATE STUDIES

KING FAHD UNIVERSITY OF PETROLEUM & MINERALS

DHAHRAN, SAUDI ARABIA

In Partial Fulfillment of the
Requirements for the Degree of

MASTER OF SCIENCE

In

MECHANICAL ENGINEERING

May 2018

KING FAHD UNIVERSITY OF PETROLEUM AND MINERALS
DHAHRAN- 31261, SAUDI ARABIA

DEANSHIP OF GRADUATE STUDIES

This thesis, written by **ABDUL-RAHMAN A.H. NOUR** under the direction of his thesis advisor and approved by his thesis committee, has been presented and accepted by the Dean of Graduate Studies, in partial fulfillment of the requirements for the degree of **MASTER OF SCIENCE IN MATERIALS SCIENCE & ENGINEERING.**

Dr. Zuhair M. Gasem
Department Chairman

Dr. Zuhair M. Gasem
(Advisor)

Dr. Salam A. Zummo
Dean of Graduate Studies

21/5/13
Date

Dr. Ihsan Ul Haq Toor
(Member)

Dr. Ime Obot
(Member)

Dedication

This is to my loving parents, my unique siblings, my brilliant wife, and God's gift Rayan.

ACKNOWLEDGMENTS

I must acknowledge King Fahd University of Petroleum and Minerals (my Alma Mater) for its supporting role in this research.

Great gratitude is due to all those who helped in my knowledge-based journey: Dr. Zuhair M. Gasem (my advisor and ME Chairman), my professors, my colleagues, the Mechanical Engineering Department, KFUPM's Center of research Excellent in Corrosion, and KFUPM.

I would also like to thank the distinguished professors of my thesis committee; Dr. Ihsan Ulhaq Toor and Dr. Ime Obot.

TABLE OF CONTENTS

LIST OF TABLES

LIST OF FIGURES

LIST OF ABBREVIATIONS

AC	:	Alternating Current
AO	:	Aesthetic Objective
ATC	:	2-amino-5-(ethylthio)-1,3,4-thiadiazole
BBMHB	:	Organic Inhibitor 2-(2-Bromophenyl)-1-methyl-1H-Benzimidazole
C_{dl}	:	Double layer capacitance
DIC	:	Dissolved inorganic carbon
DO	:	Dissolved oxygen
DPLE	:	Date Palm (*Phoenix dactylifera*) Leaf Extract
EIS	:	Electrochemical impedance spectroscopy
edl	:	Electrical Double Layer
FT-IR	:	Fourier-transform infrared Spectroscopy
ICT	:	Idiopathic Copper Toxicosis
IR	:	Infrared
KI	:	Potassium Iodide
MIC	:	Microbiological Induced Corrosion
MAC	:	Mechanically Assisted Corrosion

MPY	:	Mili-inches per year
Na_2WO_4	:	Sodium Tungstate
PCA	:	2-pyrazinecarboxamide
PDP	:	Potentiodynamic Polarization
Q_f	:	capacitance across inhibitor adsorbed film on metal surface
R_{ct}	:	charge transfer resistance
R_f	:	R_{ct} across inhibitor adsorbed film on metal surface
TDS	:	Total dissolved solids
TYV	:	Thymus vulgaris
XYA	:	Xylopia aethiopica
ZGO	:	Zingiber officinale
SEM	:	Scanning Electron Microscope

ABSTRACT

Full Name : Abdul-Rahman Abdullah Hassan Nour

Thesis Title : Date Palm Leaf Extract (DPLE) as a Green Corrosion Inhibitor for Copper in Raw Water

Major Field : Master of Science in Materials Science and Engineering

Date of Degree : May 2018

The inhibition of copper corrosion in raw water by Date Palm (*Phoenix dactylifera*) Leaf Extract (DPLE) was investigated by electrochemical and weight loss methods. A significant decrease in the corrosion rate of copper in raw water was observed in the presence of DPLE extract in the solution. The corrosion rates of copper and the inhibition efficiencies of the DPLE and 2-(2-Bromophenyl)-1-methyl-1H-Benzimidazole (BBMHB) were measured. The Inhibition efficiency of DPLE was compared to that of the commercially available organic inhibitor (BBMHB) in order to evaluate the effectiveness of DPLE in inhibiting copper corrosion in raw water. The results showed that both organic BBMHB and green DPLE inhibited copper corrosion in raw water solution with high efficiencies. The inhibition efficiency was concentration dependent. The inhibitor adsorption followed the Langmuir's adsorption isotherm. The metal surface was studied using FT-IT to analyze the functional groups that constituted this film. Synergistic behavior of DPLE was also studied using Sodium Tungstate (Na_2WO_4) and Potassium Iodide (KI). The addition of small amounts of KI to DPLE improved the inhibition efficiency of the

mixture indicating a synergistic effect. The results demonstrated that the aqueous solution of DPLE can be effectively used as an inhibitor for copper corrosion in raw water media.

ملخص الرسالة

الاسم الكامل: عبدالرحمن عبدالله حسن نور

عنوان الرسالة: مستخلص أوراق النخيل مثبط طبيعي لتآكل النحاس في المياه الجوفية

التخصص: درجة الماجستير في العلوم في علم المواد والهندسة

تاريخ الدرجة العلمية: مايو / أيار لعام 2018

تمت دراسة اثنين من مثبطات التآكل على معدن النحاس، و أولهما : طبيعي مستخلص من أوراق سعف شجر النخيل، وَالثاني هو مركب عضوي اصطناعي و أحد مشتقات البنزيمادازول الذي تستخدم مشتقاته كمثبطات تآكل للنحاس. و تمت دراسة تآكل النحاس في مياه جوفية مستخرجة من بئرجامعة الملك فهد البترول و المعادن و التي تتميزبارتفاع نسبة الملوحة فيها. و لقد تمت هذه الدراسة باستخدام بتراكيز مختلفة للمثبطات و ثلاثة طرق ، و هي: طريقة فقدان الوزن للعينات، و طريقتين من الطرق الكهروكيميائية. و بينما كانت كفاءة كلٍ من المثبطين عالية، أظهرت النتائج كفاءة عالية و قدرة مرتفعة لمستخلص أوراق سعف النخيل على تثبيط تآكل النحاس، مع تميز المستخلص بكونه غير سام و صديق للبيئة و توفره بكثرة في المملكة العربية السعودية على وجه الخصوص، و الشرق الأوسط على وجه العموم. كما تمت دراسة تأثير ارتفاع درجة حرارة المياه الجوفية، حيث تمت الاختبارات على مياه جوفية بلغت درجات حرارتها 22 و 40 و 60 درجة مئوية. و أظهرت النتائج انخفاض كفاءة تثبيط التآكل لكل من المستخلص الطبيعي و المركب العضوي الاصطناعي كلما ارتفعت درجة حرارة المياه الجوفية. كما تمت دراسة تأثير طول فترة تعرض النحاس للمياه الجوفية على كفاءة تثبيط التآكل لكل من المستخلص الطبيعي و المركب العضوي الاصطناعي. و أظهرت النتائج ارتفاع كفاءة تثبيط التآكل لكل من المستخلص الطبيعي و المركب العضوي الاصطناعي كلما زادت الفترة الزمنية التي تعرض خلالها النحاس للمياه الجوفية. و لقد توافقت النتائج التي تم الحصول عليها لطرق الفحص الثلاث على فاعلية مستخلص أوراق سعف النخيل العالية في تثبيط تآكل النحاس عند تعرضه للمياه الجوفية. كما تمت دراسة الخصائص التوافقية لمستخلص أوراق سعف النخيل عند إضافة كل من تنجستات الصوديوم (Na_2WO_4) و أيوداید البوتاسيوم (KI) له ، كلاً على حدة. و لقد أظهرت النتائج عدم وجود خصائص توافقية لمستخلص أوراق سعف النخيل مع تنجستات الصوديوم (Na_2WO_4)، و الذي سجل انخفاضاً في كفاءة التثبيط مقارنة بكفاءة كل منهما على حدة. بينما تم الحصول على كفاءة تثبيط لتآكل النحاس أعلى بكثير عند إضافة أيوداید البوتاسيوم (KI) لمستخلص أوراق سعف النخيل من كفاءة كل منهما على حدة، مما أكد بدوره وجود خصائص توافقية ممتازة بينهما.

1 INTRODUCTION

1.1 Motivation and Objectives

The cost of corrosion control and mitigation constitutes a huge part of the annual operation and maintenance cost in most industries. Since using noble, corrosive-resistant material is often neither feasible nor practical, corrosion inhibition has become the essential method that is widely used in corrosion control. This involves using corrosion inhibitors to limit metal dissolution and extend its lifespan. Most of these corrosion inhibitors, however, are neither cheap nor environmentally friendly.

Hence, it is imperative to find effective corrosion inhibitors that are green, renewable and cost-effective. Date-Palm plant was chosen for this research because it is found in abundance in Saudi Arabia, which means it is readily available for both research and future commercial implementation. Copper is a key construction material in cooling systems across the industry, and therefore it is chosen as the substrate metal for this research.

The objective of this research is to evaluate the performance and efficiency of DPLE extract as an inhibitor of copper corrosion in raw water solution.

1.2 Copper

Ever since the early days of human civilization, man has discovered metals and started relying on them for sustaining his livelihood and improving his living standards. Copper

was one of the most important metals used by man, which was later alloyed with tin to produce bronze. That announced the start of the Bronze Age at about 3000 B.C.

Copper is an important construction material. Because of its good mechanical and conductivity properties (both electrical and thermal alike), it has wide ranging applications, such as production of wire, pipes, and sheets. In today's world, Copper is used in building cooling systems in various applications (e.g. power plants, oil and gas industries, mining and petrochemical industries). Copper plays a key role in generating electric power and transmitting it thereafter. It also makes an essential part in today's heat exchangers. The automobile industry also uses copper in wiring harnesses and more so in recent hybrid vehicles.

In the last 25 years, the world has increasingly been using copper, which has subsequently driven production rates dramatically higher. As a result, recycling is increasingly becoming a favorable source of copper as nearly one-third of all copper consumed worldwide comes from recycling without losing any of the metal's chemical or physical properties.

1.3 Corrosion Chemistry

Corrosion is the dissolution of metal by reacting with the environment. Rust is one of the most commonly known forms of metal corrosion, which occurs when iron corrodes. Rust is a hydrated ferric oxide, which appears in the familiar color of red or dark brown (Figure 1). Thus, steel oxidizes (rusts and corrodes), but the non-ferrous metals such as aluminum, copper, and zinc also corrode (but do not rust) [1] and [2].

Figure 1. Rust appears on ships anchor chains [1].

Studying corrosion processes brings together chemistry, physics and materials science. However, further emphasis on the science of mechanics becomes all so necessary to better understand how mechanically assisted corrosion (MAC) occurs. Stress-corrosion cracking and corrosion fatigue are two examples of MAC.

1.3.1 The Four elements of Corrosion

There are 4 elements that must be available before corrosion can occur:

- **Anode (an electron donner):** the electrode where the anodic reaction takes place, forming positive ions and generating free charge (electrons).
- **Cathode (an electron receiver):** the electrode that receives electrons, forming negative ions and is protected from corrosion.
- **Electrolyte:** The conductor through which current is carried. Electrolytes are ionized solutions capable of conducting electricity and are generally aqueous solutions.
- **Return Current Path:** The metallic path that connects the anode to the cathode, which are often part of the same metal substrate.

Substituting a different metal for the anode or cathode may cause the direction of the current to reverse, resulting in a switch to the electrode experiencing corrosion. The galvanic series of metals will be discussed in section 1.4.3 later in this chapter.

Corrosion belongs to the field of electrochemistry as it usually occurs through the operation of electrochemically coupled half-cell reactions. As shown in Figures 2 and 3, in a half-cell, reaction electrons appear on one side or another of the reaction. A half-cell reaction can be either an oxidation or a reduction reaction [1].

If electrons are products (right-hand side of the reaction), then the half-cell reaction is an oxidation reaction. While, if electrons are reactants (left-hand side of the reaction), then the half-cell reaction is a reduction reaction.

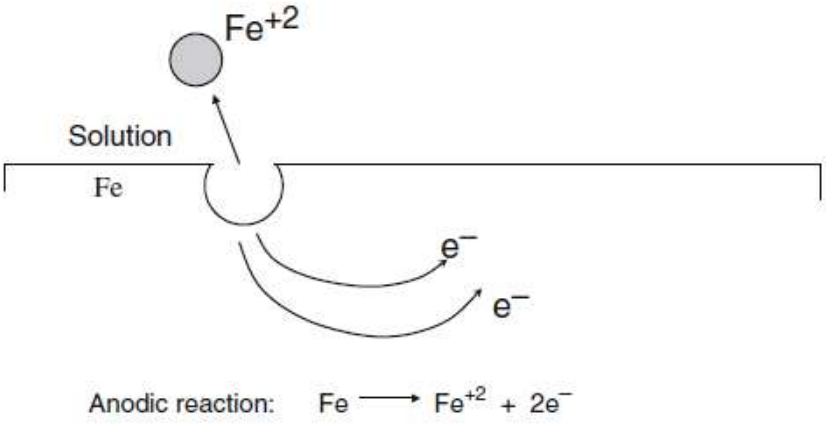

Figure 2. The dissolution of iron is an anodic reaction [1].

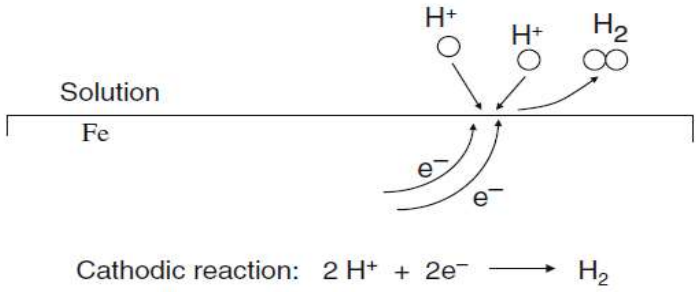

Figure 3. Hydrogen evolution on iron in an acid solution is an example of a cathodic reaction [1].

The reason that two different electrochemical half-cell reactions can occur on the same metal surface lies in the heterogeneous nature of a metal surface. Polycrystalline metal surfaces contain an array of site energies due to the existence of various crystal faces (i.e., grains) and grain boundaries. In addition, there can be other defects such as edges, steps, kink sites, screw dislocations, and point defects. Moreover, there can be surface contaminants due to the presence of impurity metal atoms or to the adsorption of ions from solution to change the surface energy of the underlying metal atoms around the adsorbate. Some of these effects are illustrated in Figure 4 [1].

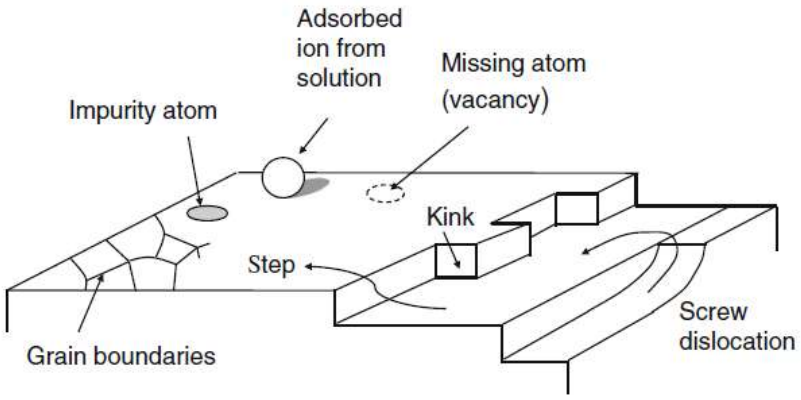

Figure 4. The heterogeneous nature of a metal surface showing various types of imperfections [1].

1.3.2 Interfaces

No matter how large an aqueous solution (electrolyte) may grow, it must terminate in a boundary with another phase. Oceans, seas and great lakes are key examples of this. Interfaces occur between different phases, and the one of essential importance to our study is the metal/solution interface and is followed closely by the solution/air interface. In the bulk of the electrolyte/solution, ions or molecules are surrounded by other ions or molecules in all directions so their arrangement is almost the same throughout the bulk. Interface regions have different characteristics, as interface ions or molecules do not have neighboring ions or molecules distributed in all directions.

1.3.3 Electrical Double Layer (edl)

While, there have been several models that describes the electrical double layer [1], one can comfortably state that for corrosion to take place, corroding cations (anode) must pass through the edl into the solution, and anions (cathode) from the solution must enter the edl in order to attack the metal. Hence, the edl controls the corrosion process. The simple equivalent circuit in Figure 5 is used to model the edl and the corrosion process as follows:

C_{dl}: *The double layer capacitance, as the edl at a metal surface is similar to a parallel plate capacitor*
R_p: *The Faradaic resistance, which represents the resistance to charge transfer across the edl*
R_s: *The ohmic resistance of the solution.*

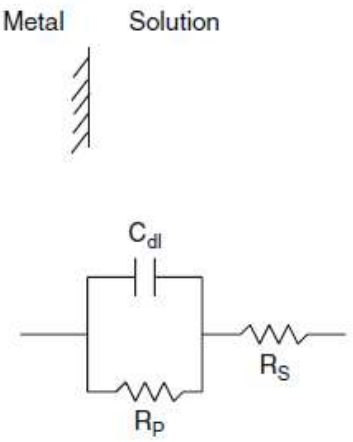

Figure 5. Simple equivalent circuit model of the electric double layer [1].

1.3.4 Corrosion Kinetics

The concept of corrosion tendency is based on thermodynamics. In practice, however, we are concerned primarily with rates of corrosion — that is, with kinetics. The potential change caused by net current to or from an electrode, measured in volts, is called polarization. Electrode kinetics is the study of reaction rates at the interface between an electrode and a liquid. The science of electrode kinetics has made possible many advances in the understanding of corrosion and the practical measurement of corrosion rates. The interpretation of corrosion processes by superimposing electrochemical partial processes was developed by Wagner and Traud [3]. Important concepts of electrode kinetics that will be introduced in this chapter are the corrosion potential (also called the mixed potential and the rest potential), corrosion current density, exchange current density and Tafel slope.

1.4 Types of Corrosion

Corrosion can be of many forms. It can be classified as the appearance of corroded metal. However, all types are interrelated. The kind of corrosive attack depends on material, system construction conditions, the scale and oxide film formation, and the hydraulic conditions [4]. The distribution of anodic and cathodic area over the corroding metal primarily influences the types of corrosion. In particular the types of corrosion that will be reviewed are uniform corrosion, pitting corrosion, galvanic corrosion, concentration cell corrosion and microbial induced corrosion.

1.4.1 Uniform Corrosion

Uniform corrosion is the type of corrosion that is most common. The corroding metal acts as both the anode and cathode. These areas are continually shifting, resulting in a smooth surface that may or may not be covered with corrosion byproducts [29]. These corrosion cells can develop on these heterogeneous metals because of possible differences in crystal structure and imperfections in metal. Also, the difference in concentrations of oxidants and reductants in solutions cause momentary differences in potentials leading to this type of corrosion [4]. Although a uniform attack is the most common form of corrosion and consumes most metals, it is also the least serious as its rate can be easily predicted and thus the life of the metal can be determined [5].

In the distribution system within a pipe when the anodic and cathodic areas are very small and close to one another uniform corrosion will occur. Anodic sites will shift about the surface resulting in a relatively uniform loss of metal over the surface of the pipe. Uniform

corrosion results from the heterogeneous nature of the metal pipe. It results in a relatively uniform loss of metal over the surface of the pipe.

For copper tubings uniform corrosion is characterized by a surface covered with a loose, powdery blue-green scale or with tarnish like an old copper penny. If the uniform corrosion rate in copper is excessive it will cause unacceptable levels of copper corrosion byproduct release resulting in green or blue water problem. This type of corrosion may cause coloring or straining of the cloth, metallic test water or in extreme case, nausea if enough copper is consumed [6]. Uniform copper corrosion rates are commonly expressed as pipe penetration rates (rate of pipe wall loss) in mili-inches per year (mpy). According to [7] if corrosion rate is more than 1mpy it is considered high and if it is less than 1mpy it is low.

1.4.2 Pitting Corrosion

Pitting is a form of extremely localized attack that results in holes in the metal [8]. It is indeed one of the most pernicious, and damaging forms of corrosion and very difficult to predict. It can cause failures with only a small percentage weight loss of the entire structure. A local cell or the formation of an anode is necessary for all corrosion by electrolytes. These cells are created because of differences in the metal surface or in the environment. Impurities, grain boundaries, nicks and rough surfaces are all metallurgical or mechanical differences, while concentration cells are environmental differences. The smaller the anodic area is relative to the cathode, the more severe the corrosion will be [8].

Pitting can begin or concentrate, at a point of surface imperfections, scratches, or surface deposits in a pipe. It is frequently caused by ions of a metal higher in the galvanic series

plating out on the pipe surface. Pitting occurs in an environment that does not offer comprehensive protection but rather an incomplete one. The pit develops at a localized anodic point on the surface and continues by virtue of a large cathodic area surrounding the anode [4].

The initiation of pitting in copper tubing is not well understood. Lucey's [9] membrane theory is the most widely used explanation of this mechanism. According to this mechanism the key to pit initiation is the formation of porous cuprous oxide membrane over a cuprous chloride layer lying adjacent to the copper surface. A cuprous chloride film is formed immediately when copper is immersed in solution containing chloride ion. The cuprous chloride is removed from the surface by hydrolysis to cuprite, oxidation and formation of cupric salts, and ultimately dissolution in bulk solution. The removal of cuprous chloride forms passivating scale on the copper. However, in unusual case the formation of cuprous chloride may exceed the removal, which results in cuprous chloride formation under the cuprite and initiation of pitting in copper.

The galvanic couple between the copper and the carbon surface is another factor that increases the pitting [10]. Carbon films are cathodic to the copper metal so it stimulates the copper corrosion. Galvanic corrosion in distribution systems occurs where brass, bronze, or copper is in direct contact with aluminum, galvanized iron, or iron. Proper selection of materials and the order of their use in domestic hot- and cold-water plumbing systems are critical to the control of corrosion. Galvanic corrosion rates can be increased by having large cathodic areas relative to anodic areas, the physical closeness of the two metals. It also depends on how further apart the two metals are on the galvanic series. To prevent

galvanic corrosion, for example, only copper tubing should be used with copper-lined water heaters. Brass valves in contact with steel and galvanized plumbing in waters with high total dissolved solids cause corrosion of the steel and galvanized pipes. Dissolved copper can attack spots on galvanized pipe, thereby causing copper-zinc galvanic cells [11].

1.4.3 Galvanic Corrosion

As two different types of metals or alloys come into contact each other, galvanic corrosion occurs such that the elements of a corrosion cell are present. One of the metals serves as the anode (loses valance electrons) and deteriorates, while the other serves as the cathode (receives electrons). Metals can be arranged in order of their tendency to become anodic and this is called the galvanic series [4]. An empirical galvanic series of metals is shown in Figure 6. The further two metals in contact are apart in the galvanic series, the greatest the potential for corrosion.

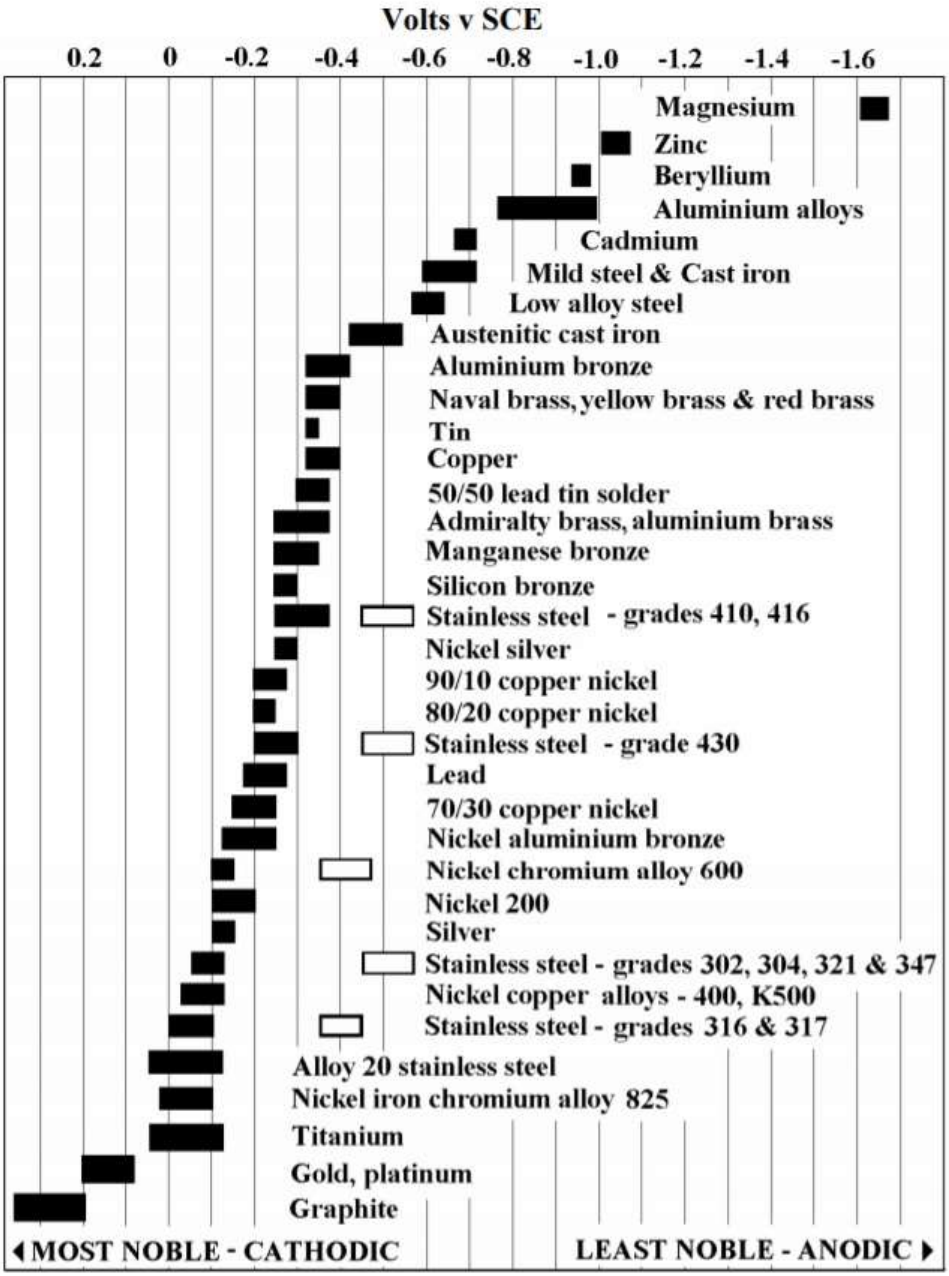

Figure 6. Galvanic Series Chart

1.4.4 Microbiological Induced Corrosion

Microbiologically induced corrosion (MIC) results from a reaction between the pipe material and organisms such as bacteria, algae, and fungi [4]. The corrosion in the distribution system can be affected by the microorganisms in numerous ways. Some microorganisms are able to metabolize corrosion inhibitors or protective coatings. Oxygen concentration cells can be created by aerobic microorganisms on the metal surface. Uneven depletion of oxygen occurs due to the variations in biofilm density and thickness, which ultimately creates areas that are more anodic then others. Formation of ionic concentration cells can be enhanced by microbial activity. MIC in case of copper is very important. According to different investigators [12] the developments of pitting in new hospitals in Germany and Scotland in the mid-1980s were due to the microbial activities. It also shows that excessive copper corrosion by product release occurs in the extremities of the system with very low Chlorine residual. From these studies it is suspected that the dominant cause of corrosion in these cases may be microbial activities. The possible mechanism behind the MIC can be summarized as:

1. Creation of a zone of lower pH surrounding the metal surface due to production of acidic metabolites on the metal surface
2. the binding of copper by extracellular polymeric substances (EPS) of microbial origin.
3. Change of the nature and porosity of the oxide film from the incorporation of cells and polymers.

Biofilm activities can also result in changes in interfacial chemistry causing a destabilization in the passive film or prevention of formation of the passive film on the copper surface.

1.4.5 Concentration Cell Corrosion

Concentration cell corrosion is similar to uniform corrosion. However instead of dissimilar metal, a galvanic current can also be set up when a single metal is exposed to different concentrations (ionic strengths) of water solutions. As a result, anodic and cathodic areas are formed, and corrosion occurs [8]. Variations in pH, metal-ion concentration, anion concentration, or dissolved oxygen promote atom dissolution and caused by differences in the solution potential of the same metal. Differences in temperature can also induce differences in the solution potential of the same metal [4]. Concentration cells are the usual cause of the troublesome local etches or pitting type of metal loss.

Concentration cell corrosion can occur at metal-water interfaces exposed to air, such as in a full water tower, accelerating corrosion a short distance below the surface. The dissolved oxygen (DO) concentration is replaced by diffusion from the air and remains high at and near the surface but does not replenish as rapidly at lower depths because of the distance. Therefore, the corrosion does not take place at the surface but rather at a level slightly below the surface.

1.5 Physical Factors Affecting Corrosion in water systems

The physical, chemical and biological characteristics of water affects the occurrence and rate of corrosion [4]. These factors are interrelated so in most cases corrosion is caused or

increased by a complex interaction among several factors. The corrosion in water distribution systems depends upon the water composition and composition of the pipe material. Flow velocity and temperature are the two main physical characteristics of water that affect corrosion.

1.5.1 Velocity

Corrosion of pipe material is always affected by the velocity of the water it carries. High velocities increase the rate at which dissolved oxygen comes in contact with the pipe materials, thus increasing the corrosion. Erosion corrosion is mainly caused by high velocities [4]. M.F. Obrecht and L.L. Quill [13] found that the corrosion in copper tubing by sodium zeolite softened water increases with increasing velocities. However, high velocities can have a beneficial effect on corrosion by formation of protective coating at faster rate due to high velocity transportation of the protective material to the surfaces occurs at a higher rate.

1.5.2 Temperature

Increases in temperature should increase the rate of corrosion because for every 10°C rise in temperature, chemical reaction rates tend to double. Moreover, the electrode potential is proportional to the absolute temperature [4]. But in practice, this rule is not always observed as there are other factors that affect corrosion. The effect of temperature varies depending on the water characteristics. M.F. Obrecht and L.L. Quill [13] reported that in the case of copper an increase of temperature usually increases corrosion. I. Singh and D.S. Mavinic [14] conducted a survey on high rise residential plumbing and found that cold

water copper pipe corrosion by product is about one third of that for hot water copper pipes. D.M. Macquarrie et al. [15] also reported lower copper corrosion at lower temperature. Nevertheless, several researchers [6], [15], [16] and [17] reported that with increase of temperature the copper corrosion decreases especially when type III soft water pitting or blue water occurs. They reported that at high temperature (65°C) copper corrosion reduced markedly. They found highest corrosion rate at temperature 30°C. They propose that the elevated temperature may kill the microorganism that cause corrosion because most bacteria flourish at temperature range 25 to 45° C.

1.6 Chemical Factors Affecting Corrosion in water systems

Dissolved substances in water have an important effect on corrosion. Several of these chemical factors arc closely related, and a change in one can impact another.

1.6.1 pH

The pH of water is a measure of acidity from H^+ concentration. The pH is an important factor in corrosion because hydrogen ions (H^+) are one of the major substances that accept the electrons released by a metal when it corrodes. Most drinking water's pH ranges from 6 to 10. With the increase of pH, the corrosion rate decreases. One common corrosion control treatment strategy is to increase the pH of the source water. This can be done through chemical (dosing) or non-chemical means. Any increase in pH within the pH range of 5 to 10 shall result in a decrease in copper levels. At the higher pH levels, copper has less tendency to dissolve and enter drinking water. The formation or solubility of protective films is also pH dependent [4]. The water pH varies widely as it travels through the

distribution network. Although the pH measured at the pump station or treatment facility may appear to be stable, as it passes through the distribution system it may increase or decrease significantly. This will depend on the size of the distribution system, flow rate, age and type of plumbing material.

1.6.2 Alkalinity and Dissolved Inorganic Carbon

Alkalinity is a measure of the ability of water to neutralize acids; it is a measure of buffering capacity against a pH drop [18]. Total alkalinity is the sum of bicarbonate, carbonate and hydroxide ions. Alkalinity is typically reported as mg/L "as calcium carbonate" ($CaCO_3$). Dissolved inorganic carbon (DIC) is defined as the sum of all dissolved carbonate containing species [4]. It is measured as milligrams of carbon per liter (mg C/L). DIC is related to alkalinity and if pH and alkalinity are known then DIC of the water can be predicted. The presence of bicarbonates and carbonate impacts many key reactions in corrosion chemistry, including the water's ability to form a protective metallic carbonate scale or passivating film [4]. At a constant pH, copper levels increase as the DIC increases, the effect of DIC is strong as the effect of pH at high (> 30 mg C/L) levels of DIC. Increases in DIC of 3-6 mg C/L will typically have minimal impact on copper levels, particularly with respect to the regulatory action level. However, M. Edwards and J. F. Ferguson [16], showed that bicarbonate ion have a dual nature that is pH dependent. The researcher found that at pH<7.0 it causes activation i.e. increase corrosion and at pH>8.5 it causes passivation i.e. reduces copper corrosion. In contrast, for control of lead, as the DIC increases the lead concentration decreases or remains essentially unchanged within the pH

range of about 7.0 to 8.0. The effect of DIC usually is more prominent at lower pH than at higher.

1.6.3 Dissolved Oxygen

Oxygen is one of the most prevalent agents of corrosion. In many cases it is the substance that accepts the electrons given up by the corroding metal [15]. However, the addition of dissolved oxygen may have a great effect on water quality as it causes dissolved reduced iron and manganese to oxidize (more slowly) forming more soluble copper compounds than waters with no dissolved oxygen. This calls for more consideration and control of aeration in order to mitigate corrosion control and reduce metal oxidation. A balanced approach towards carbon dioxide removal and pH rise from aeration must be weighed against the possibility of creating soluble copper in the distribution system from increased dissolved oxygen addition.

1.6.4 Disinfectant Residual

Several researchers investigated the effect of disinfectant on copper corrosion. [19] tested chlorine cone, of 1,2,5,7.5,10 mg/L for 24-hour exposure and found that a higher concentration of free chlorine causes more copper dissolution especially at lower pH. [20] also reported similar trends from their field study reported about two similar buildings, where copper by-product release was higher at the building with higher chlorine level. Also [19] concluded that chlorine is dominant over oxygen as an oxidizing agent on copper. In contrast to these findings [16] found that chlorine residual reduces copper corrosion. They concluded that chlorine might prevent the usual “blue water” or the soft-water pitting

problem. Also several other researchers also reported that in New Zealand, Australia, and US excessive by-product release in chlorinated water supply occurs at very low residual chlorine (CI2) concentration.

1.6.5 Corrosion Inhibitors

Most well-known organic inhibitors are compounds that contain different atoms such as nitrogen, oxygen or sulphur and multiple bonds, that allow its adsorption on the metal surface. By adsorption mechanism of the inhibitor molecules on the metal surface, these compounds create a mono or multilayers barrier that adsorbs onto the metal substrate [21] [22].

Phosphate inhibitors are usually used for corrosion control in the distribution system. Poly phosphate or orthophosphate or a blend of these two is used as corrosion inhibitor. Though researchers have studied the effect of phosphate inhibitor on corrosion, how these inhibitors actually work is not clearly known. D.A. Bancroft [23] reported that for tap water with low pH, alkalinity and hardness 0.5 mg/L zinc ortho-phosphate reduced copper corrosion. Stone et al. [20] and Boffardi et al. [24] also conducted copper pipe rig test with orthophosphate and found similar effect. However, Edwards Eet al. [25] reported that poly or orthophosphate general reduced the soluble copper concentrations, but orthophosphate is more efficient than polyphosphate. They also reported that at pH 7.2 and alkalinity 300mg/L polyphosphate significantly increased copper release by hindering malachite formation.

1.7 Corrosion Mitigation and Control

Corrosion scientists and engineers have strived to devise and implement mitigation and control plans to best manage corrosion and reduce its impact. The following areas have been identified as key elements of any corrosion mitigation and control plan:

- **Design:** The design process entails several elements:
  - Process Parameters (temperature, velocity, pressure, chemistry)
  - Material Selection
  - Geometry for drainage
  - Corrosion Allowance
  - Crevices
- **Protective Coatings:** the use of coatings breaks the pathway of ion, molecule and/or charge transfer and hence stops corrosion
- **Cathodic Protection (CP):** Cathodic protection is a technique that controls corrosion by turning the anode into a cathode. This can be done using:
  - **Sacrificial anode:** is connected to the metal to be protected to act as the anode.
  - **Immersed current:** an external DC source provides enough current to protect metal structures such as long pipelines.
- **Modification of Environment:**
  - Corrosion inhibitors
  - pH

2 LITERATURE REVIEW

Current environmental requirements call for green corrosion inhibitors, which has created a growing interest in the use of natural products such as leaves or seeds extracts. Recent research has focused on developing green corrosion inhibitors that have good inhibition efficiency but with a lower risk of environmental pollution [26]. Corrosion scientists and researchers have hence focused on plant extracts in order to study their respective inhibition efficiency. As green products, most plant extracts may serve as a source of non-toxic, eco-friendly, inexpensive, readily available and renewable source inhibitors for preventing metal corrosion [26] [27] [28].

Many researchers have reported on the use of green products for mild steel corrosion inhibition in various corrosive media [29] [30] [31], but only fewer examples of copper corrosion inhibition were reported [30], [32], and [27]. Umoren et al. investigated using Date Palm Seed Extract (DPSE) [33] and Date Palm Leaf Extract (DPLE) [34] to inhibit the corrosion of mild steel in acidic media, and the results were positive and promising as shown in Figure 7 below. This work, therefore, reports on comparing the use of Date Palm Leaf Extract (DPLE) and 2-(2-Bromophenyl)-1-methyl-1H-Benzimidazole (BBMHB) to inhibit the corrosion of copper in raw water media obtained from KFUPM. BBMHB was chosen as a benchmark inhibitor because it is from the family of azoles, which are excellent corrosion inhibitors for copper substrates [35].

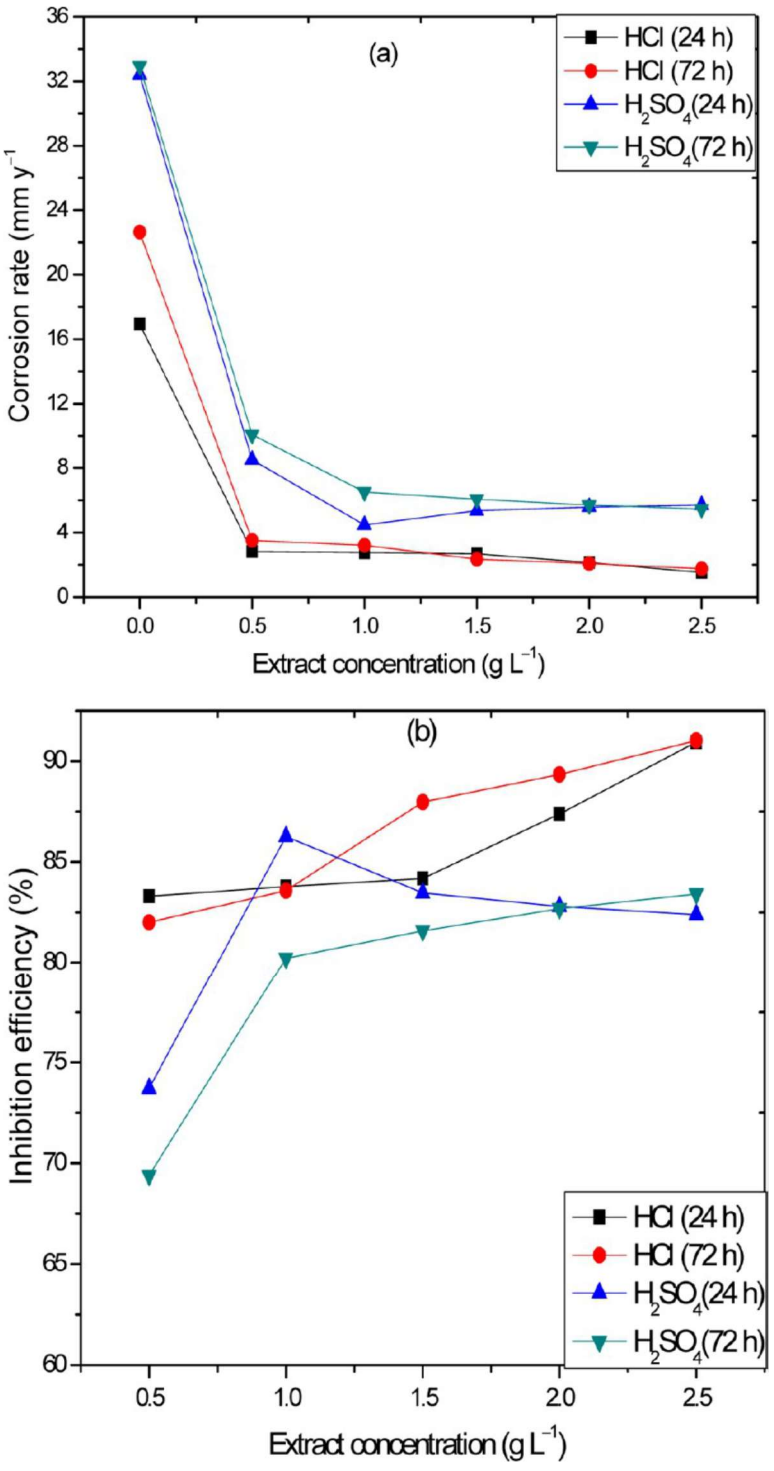

Figure 7. Plots of the (a) corrosion rate and (b) inhibition efficiency against the concentration of Date Palm Seed Extracts (green inhibitor) at different immersion times for mild steel in 1 M HCl and 0.5 M H_2SO_4 from weight loss measurements.

Kalaiselvi et al. [36] tested Artemisia pallens extract as a corrosion inhibitor for mild steel in HCl medium using weight loss measurements and electrochemical methods with good results. Their experiments concluded that the corrosion rate of mild steel in HCl medium decreased as the concentration of Artemisia pallens extract increased as shown in Figures 8 and 9.

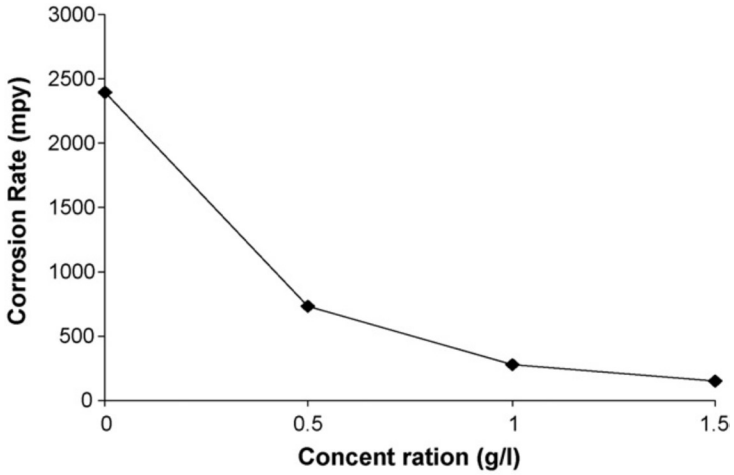

Figure 8. Corrosion rate of mild steel is inversely proportional to inhibitor concentration when exposed for 24 h in HCl medium.

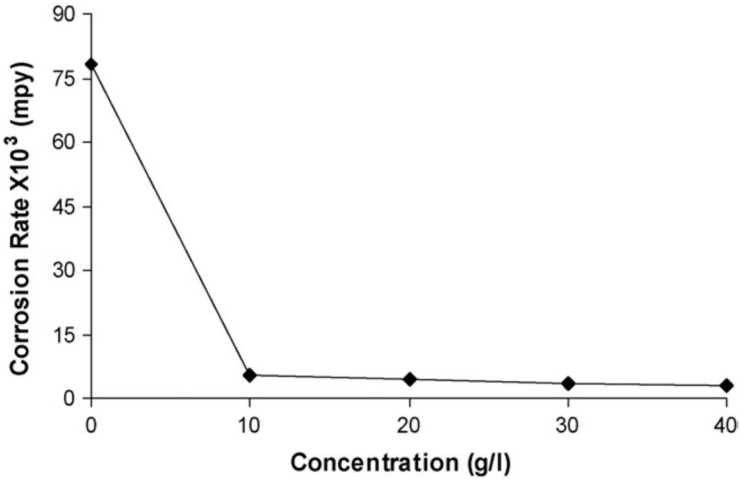

Figure 9. Corrosion rate of mild steel decreases as inhibitor concentrations increase in HCl medium for 20 min.

Krishnaveni and Ravichandran [37] studied inhibiting copper corrosion in Sulphuric acid medium using Morinda tinctoria extract. The results were positive and encouraging as the corrosion rate decreased when using the Morinda tinctoria extract. Moreover, they deduced that the corrosion rate was inversely proportional to the extract concentration. The equivalent circuit used in this study is shown in Figure 10 is in line with electric double layer model (edl) that was previously discussed in section 1.3.3. EIS and PDP plots are shown in Figures 11 and 12, respectively.

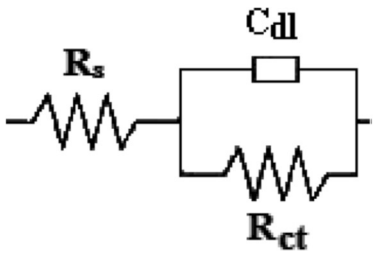

Figure 10. Randles equivalent circuit used to for the study inhibiting copper corrosion in Sulphuric acid medium using Morinda tinctoria extract.

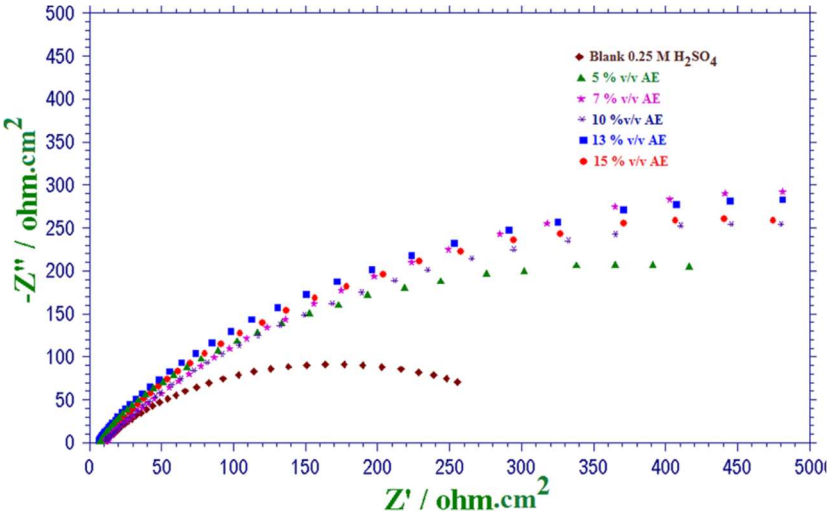

Figure 11. Nyquist plots for the corrosion of Cu in 0.25 M H_2SO_4 with various concentrations of Morinda tinctoria extract.

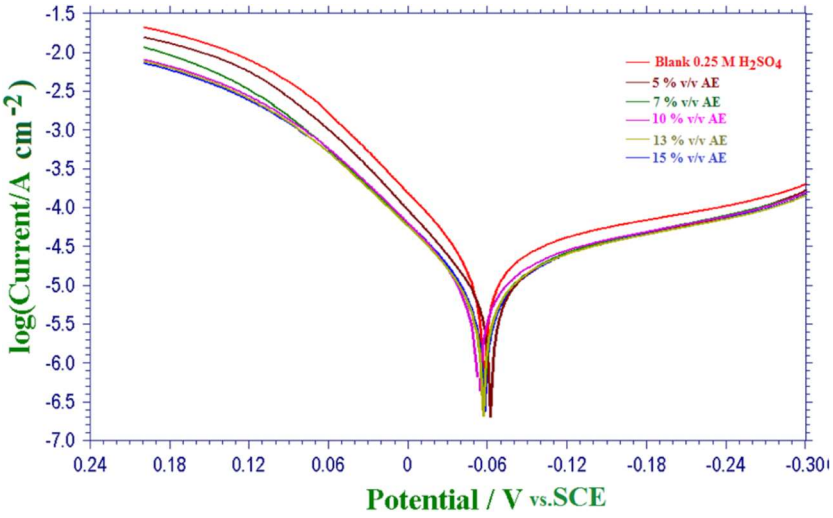

Figure 12. Tafel plots for the corrosion of Cu in 0.25 M H_2SO_4 with various concentrations of Morinda tinctoria extract.

Shah Et al. [38] investigated the inhibition of copper corrosion by mangrove tannin in aqueous 0.5 M hydrochloric acid solution using weight loss method, potentiodynamic polarization, and electrochemical impedance spectroscopy (EIS). The results obtained in this research were quite positive and promising. Moreover, the results obtained via electrochemical measurements were in good agreement with those obtained by using the weight loss method.

Senthooran et al. [39] also researched inhibiting copper corrosion using tea leaves extract in acidic medium. The results showed that tea leaves extract produce good inhibition efficiency in HCl medium of low concentrations (below 0.05 mol per dm^3). This was attributed to the adsorption of inhibitor components in the tea leave extract to the copper substrate, which confirmed to the Langmuir adsorption isotherm.

Okafor et al. [40] had earlier researched the inhibitive action of the corrosion of mild steel in sulphuric acid solutions by ethanol extracts of Thymus vulgaris (TYV), Xylopia

aethiopica (XYA) and Zingiber officinale (ZGO). The results obtained showed that the ethanol extracts of from TYV leaves, XYA fruits and ZGO roots inhibit the corrosion of mild steel in H_2SO_4 solutions. This inhibition was attributed to adsorption of their phytochemical constituents onto mild steel surface. The data fitted into the Langmuir adsorption isotherm.

Al-Dokheily et al. [41] research results on the fruit extract of Citrullus colocynthis revealed that this plant extract was an effective inhibitor on copper corrosion, with a better efficiency in acidic mediums than in alkaline and salt mediums.

El-Sayed M. Sherif [42] researched the effect of 2-amino-5-(ethylthio)-1,3,4-thiadiazole (ATD - a benzimidazole derivative) on the inhibition of copper corrosion in 3% NaCl solutions. The results showed that ATD molecules are strongly adsorbed on the copper surface preventing it from being easily corroded. EIS measurements revealed that the charge transfer resistance increased due to the presence of ATD, and this effect increased with oxygen content in the solution. Weight loss measurements showed excellent inhibition efficiencies of 83% and 94% with 1.0 mM and 5.0 mM of ATD concentrations, respectively. Results from different techniques were consistent with each other, and showed that ATD to be a good mixed-type inhibitor for copper corrosion with inhibition efficiency increasing in the order of oxygenated > aerated > de-aerated 3% NaCl solutions.

The synergistic effect of KI and 2-pyrazinecarboxamide (PCA) was studied by AA Farag and TA Ali [43]. PCA and KI inhibited the corrosion of carbon steel in 0.5 M H2So4 solution and the inhibition efficiency increased with an increase in inhibitor concentration and increased further in the presence of PCA/KI mixture. There was synergism between

PCA and KI, and the values of synergism parameter (S) were higher than unity, which suggested that there was a cooperative mechanism between the iodide anion and PCA cations.

V.S. Saji, and S.M.A. Shibli [44] researched the inhibition efficiency of individual sodium silicate, sodium tungstate and their synergistic combinations on carbon steel by several independent techniques. All combinations of these compounds exhibited higher inhibition efficiencies than did either of the individual inhibitors. FTIR spectra confirmed that the metal oxide layer, incorporating the tungstate and silicate ions was the primary cause of effective inhibition.

M.M. Solomon et al. [45] researched the synergistic inhibition of chitosan and KI on steel corrosion in 15% H2SO4 solution. The results exhibited higher inhibition efficiencies than did either of the individual inhibitors.

3 THE RESEARCH OBJECTIVES

1) To evaluate inhibition performance of DPLE as a green inhibitor and compare it to a commercially available organic inhibitor (BBMHB) for copper corrosion in raw water system.
2) To study and assess the effect of temperature (22-40-60° C) on the inhibitive performance of the two inhibitors.
3) To evaluate the effect of immersion time (24 and 72 h) on the corrosion inhibition efficiency of DPLE and BBMHB at different concentrations at room temperature.
4) To investigate the adsorption process of the inhibitors on copper substrate and suggest the appropriate adsorption isotherm.
5) To study the copper metal surface using FT-IR and SEM in order to learn more about the protective film forming on the metal surface.
6) To study possible synergistic behavior of DPLE with Na_2WO_4 and KI.

4 EXPERIMENTAL PROCEDURE

4.1 Material

Copper test coupons were cut into 25 mm x 20 mm x 5 mm dimensions for weight loss measurement. These coupons were mechanically abraded silicon carbide abrasive paper (from grade # 320 to 800), rinsed with ethanol, placed in an ultrasonic acetone bath for about 5 min to remove possible residue of polishing, rinsed with acetone, dried in warm air and then stored in moisture-free desiccators prior to use. The density of copper was taken as: 8.96 $g.cm^{-3}$.

4.2 Plant Material (Green Inhibitor)

Date-palm (*Phoenix dactylifera*) leaves were washed clean, dried in the shade for 2 days, then placed in a furnace at 60°C for 48 h and ground. Powder was then extracted in 250 ml of ethanol for 24 hours. Then, it was filtered and concentrated using BUCHI Vacuum Rotary Evaporator to remove the ethanol solvent. The residue was then dried in a vacuum oven. The elemental composition of Date-palm (*Phoenix dactylifera*) leaves was studied and researched by Saeed et al. [46] and findings were as listed in tables 1 and 2.

Table 1. Elemental Composition of Date-palm leaves

Material	**C(%)**	**O(%)**	**Na(%)**	**Mg(%)**	**Al(%)**	**Si(%)**	**Ca(%)**
Date-Palm Leaves	43.29	52.98	1.86	0.26	0.30	0.37	0.68

Table 2. Chemical Composition of Date Palm Leaves

No.	Chemical Composition	Percentage (%)
1	Holocellulose	61.63
2	Cellulose	39.00
3	Hemi Cellulose	22.63
4	Klason Lignin	15.34
5	Acid Insoluble Lignin	0.04
6	Ash	2.06
7	Soluble in hot water	12.12
8	Soluble in cold water	3.02
9	Soluble in 1% NaOH	12.2

4.3 Organic Inhibitor (BBMHB)

2-(2-Bromophenyl)-1-methyl-1H-Benzimidazole (BBMHB is a heterocyclic, aromatic, organic compound. This bicyclic compound structure is shown in Figure 13 and consists of the fusion of benzene and imidazole. Zhang et al. [35] investigated cooper corrosion inhibition using three benzimidazole derivatives (from the family of azoles) in aerated hydrochloric acid solution. These were known to work efficiently to mitigate copper corrosion in neutral/alkaline solutions. The results supported that the benzimidazole derivatives are effective corrosion inhibitors for copper in acidic solutions.

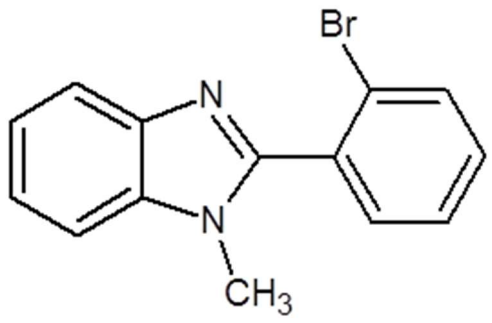

Figure 13. Structural formula of 2-(2-Bromophenyl)-1-methyl-1H-Benzimidazole (BBMHB).

4.4 Solution

All experiments were conducted using raw water from KFUPM with the addition of each inhibitor at a time (DPLE and BBMHB). Total dissolved solids weight (TDS) and pH were measured and included in the research results as shown in Table 3. Brackish water is water that has salinity more than fresh water, but not as much as saline water. Water from 3,000-10,000 mg/l TDS will be considered brackish. Hence, KFUPM raw water is brackish with 4,300 to 4,800 mg/l TDS.

Table 3. The chemical analysis of KFUPM raw water that was used as a solution in all experiments.

Analysis	**Raw Water**
pH	7.16
TDS, mg/l	4300
Electrical Conductivity, µS/cm	5540
Total Hardness, mg/l as $CaCO_3$	1160
Calcium Hardness as $CaCO_3$	800
Mg-Hardness as $CaCO_3$	360
Total Alkalinity, mg/l as $CaCO_3$	190
Chloride, mg/l as Cl^-	1410
Total Iron, mg/l as Fe	0.06
Calcium, mg/l as Ca^{++}	320
Magnesium, mg/l as Mg^{++}	86.4
Sulphate, mg/l as SO_4^{2+}	376
Silica, mg/l as SiO_2	24
Sodium, mg/l as Na^+	663
Total Suspended Solids	3
Turbidity	2
Phosphate	0.1

4.5 Weight loss measurements

Copper test coupons were cut into 25 mm x 20 mm x 5 mm dimensions for weight loss measurement. These coupons were mechanically abraded using silicon carbide abrasive paper (from grade # 320 to 800), thoroughly cleaned then weighed. Then, the samples were immersed for 24 h in 350 mL of inhibited solutions (by each inhibitor) at 22°C. Tests were performed under total immersion in naturally aerated and unstirred conditions in the absence and presence of the inhibitor and under open atmosphere. These copper coupons

were cleaned and weighed were freely hung in the different test solutions. At the end of experiments, the specimens were cleaned according to ASTM G-31 and reweighed using a digital analytical balance with a sensitivity of 0.1 mg [27]. The weight loss was calculated as the difference between the weight at a given time and the initial weight of the coupon. The standard deviation values among parallel triplicate experiments were found within 5 per cent, indicating good reproducibility. In each experiment, triplicate samples were used to validate the results. The average weight loss of three copper test coupons was obtained. From the weight loss values, corrosion rates in terms of thickness loss (mmy^{-1}) were computed using the equation:

$$C_R\ (mmy^{-1}) = \frac{87600 \times \Delta W}{\rho A t} \qquad (1)$$

where,

C_R : *The corrosion rate in terms of thickness loss(mmy^{-1})*
W : *The average weight loss (mg)*
ρ : *The density of copper ($g.cm^{-3}$)*
A : *The surface area of the specimen (cm^2)*
t : *The exposure time (sec)*

4.6 Tafel Polarization Measurements

Electrochemical testing was carried out in a conventional three electrode cylindrical glass cell connected to Gamry Instrument potentiostat/galvanostat/ZRA (Reference 3000) with a Gamry framework system based on ESA410. Gamry applications includes software DC105 for corrosion, EIS300 for EIS measurements, and the Echem Analyst 6.0 software package for data fitting. The working electrode was in the form of a rectangular cut from pure copper. A saturated calomel electrode (SCE) and platinum electrode were used as

reference and auxiliary electrode, respectively. All potentials were measured versus the SCE reference electrode. Tafel curves were obtained by changing the electrode potential automatically from −250 to +250 mV versus the open-circuit potential (E_{corr}) at a scan rate of 1mV/s. The test solution is aerated raw water in the cell inhibited with each inhibitor, one at a time with one concentration [33].

4.7 Electrochemical Impedance Spectroscopy (EIS)

EIS Electrochemical methods based on alternating currents can be used to obtain insights into corrosion mechanisms and to establish the effectiveness of corrosion control methods, such as inhibition and coatings. Electrochemical impedance was measured by applying an AC potential to an electrochemical cell and then measuring the current through the cell. Applying a sinusoidal potential excitation was assumed. EIS measurements were carried out under potentiostatic conditions in a frequency range from 100 kHz to 100 MHz, with an amplitude of 10 mV peak-to-peak, using an alternating-current (AC) signal at E_{corr} using a Gamry Instrument potentiostat/galvanostat/ZRA (Reference 600/3000) [34].

By definition, electrical impedance is the resistance to the flow of alternating electrical current (AC) when a minute amplitude sinusoidal excitation signal is applied across the system. The applied potential (E) is directly related to the values of the measured current (I) (via Equation 2 for simple circuits) but deviates slightly and becomes non-linear in complex AC circuits; impedance thus becomes the only quantity that defines the resistance of current flow in this system.

$$R = {}^{E}/_{I} \qquad (2)$$

Across an electrochemical cell, the pseudo-linear current response is gradually measured across a defined range of frequencies, since it shifts in phase (∅) once a small amplitude perturbation has been applied. The potential (E) and current response (I) are now expressed in Equations 3 and 4, derived from Randles equivalent circuit:

$$E_t = E_o \sin\ (\omega t) \tag{3}$$

$$I_t = I_o \sin\ (\omega t + \emptyset) \tag{4}$$

Where E_o and I_o are the amplitudes of applied potential and current response, respectively, while ω is the angular frequency measured in radians per second (defined as $2\pi f$); ∅ and f are the phase separation/shift and the frequency of phase, respectively.

On the Nyquist Plot the impedance can be represented as a vector (arrow) of length |Z|. The angle between this vector and the X-axis, commonly called the “phase angle”. Nyquist Plots have one major shortcoming. When you look at any data point on the plot, you cannot tell what frequency was used to record that point. The Nyquist Plot in Figure 14 results from Randles equivalent electrical circuit. The semicircle is characteristic of a single "time constant". Electrochemical impedance plots often contain several semicircles. Often only a portion of a semicircle is seen.

Another popular presentation method is the Bode Plot. The impedance is plotted with log frequency on the X-axis and both the absolute values of the impedance ($|Z|=Z_0$) and the phase-shift on the Y-axis. The Bode Plot for Randles equivalent electric circuit is shown in Figure15. Unlike the Nyquist Plot, the Bode Plot does show frequency information.

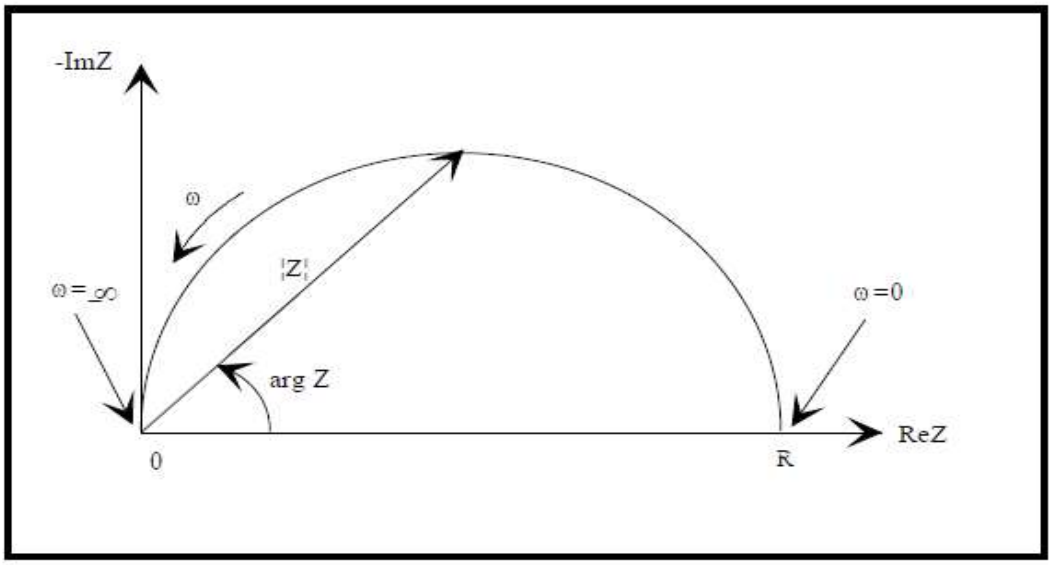

Figure 14. Typical Nyquist Plot.

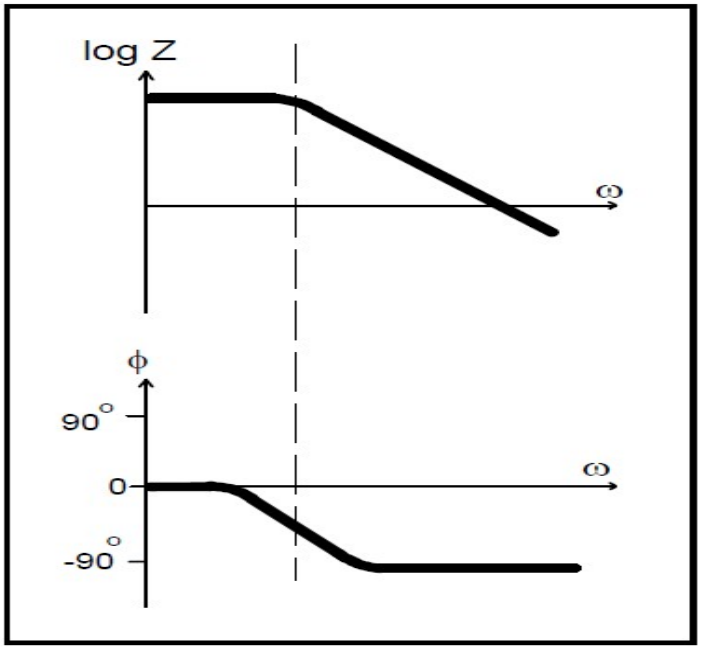

Figure 15. Typical Bode Plot.

4.8 The Effect of Temperature

Temperature has a great effect on the corrosion rate, which was studied using weight loss measurements performed in a glass reaction vessel containing 350 mL of test solution maintained at 22°C, 40°C and 60°C using a thermostatically controlled water bath provided with a thermostatic control of ±0.5° C. For the determination of effect of temperature, the test coupons were retrieved after 24 h at the three temperatures and the average weight loss of three copper test coupons was obtained.

4.9 The Effect of Time

To determine the influence of immersion time on the corrosion inhibition process, the copper specimens were retrieved after 24, and 72 h at 22°C; thoroughly cleaned using a chemical method for cleaning rust products. The results obtained for each inhibitor at different concentrations were studied for each time interval.

4.10 Metal Surface Analysis

Surface characterization of copper specimens was carried out using scanning electronic microscope (SEM), after exposure to DPLE green inhibitor.

Analysis of FT-IR spectra was used to analyze DPLE powder and the corroded copper sample in raw water inhibited by DPLE. Organic compounds exposed to electromagnetic radiation can absorb energy of only certain wavelength (unit of energy) and transmits energy of other wavelengths. Changing wavelengths to determine which ones are absorbed and which are transmitted produces as absorption spectrum [37].

5 RESULTS AND DISCUSSION

In this study, the performance of Date Palm Leaf Extract (DPLE) was tested as a corrosion inhibitor for copper metal in a raw water solution using weight loss measurements and electrochemical methods. Those tests were repeated using one of the benzimidazole derivative compounds (BBMHB), widely used and known to be effective copper corrosion inhibitors. Test results of the green DPLE inhibitor were then compared to those of BBMHB organic inhibitor. The obtained data were studied and graphically analyzed using adsorption isotherms. The data and results will be thoroughly discussed in this chapter.

5.1 Weight loss measurements for 24 and 72 h

The weight loss data were collected for three batches of copper test samples after 24 and 72 h immersion in raw water at 22°C with different concentrations of DPLE and BBMHB. Each concentration was tested 3 times in order to validate the collected weight loss data. The collected weight loss data were used to determine the corrosion inhibition efficiency of DPLE and BBMHB at different concentrations. The results were presented in Tables 4 to 9, and then average inhibition efficiencies were plotted in Figures 16 to 19 against different concentrations of inhibitors.

Results showed that the inhibition efficiency of organic BBMHB was higher than that of green DPLE at equal concentrations. Nevertheless, the addition of DPLE significantly reduced the corrosion rate of copper compared to uninhibited raw water. Inhibition efficiency proportionally increased with increasing inhibitor concentration.

The increase in the inhibitive action with the increase in inhibitor concentration can be ascribed to the blocking of the active sites of the metal surface. DPLE inhibition efficiency was studied using weight loss measurements and recorded a high performance between 70 and 80% when DPLE concentration was higher than 1000 ppm. Unlike organic commercial inhibitors, DPLE is abundantly available and relatively cheap and hence high concentrations do not cost much at all.

Results also showed the effect of immersion time on the inhibition efficiency. This will be discussed further in section 5.5.

Table 4. Corrosion rate calculated from weight-loss data of copper in raw water and inhibition efficiency as a function of inhibitor concentration in 24 h immersion at 22° C – Batch 1.

Inhibitor Concentration (ppm)	**Initial Weight** (g)	**End Weight** (g)	**Lost Weight** (g)	**Corrosion Rate** (mmy^{-1})	**Inhibition Efficiency** (%)
Blank	20.6835	20.6823	0.0012	0.03533	-
DPLE 160	20.7382	20.7372	0.001	0.02703	22%
DPLE 320	22.772	22.7711	0.0009	0.02433	36%
DPLE 800	22.5492	22.5485	0.0007	0.02014	55%
DPLE 1000	20.2298	20.2293	0.0005	0.01430	70%
DPLE 2000	20.2291	20.2288	0.0003	0.00858	78%
BBMHB 800	23.11	23.1096	0.0004	0.01107	78%
BBMHB 1000	20.7451	20.7448	0.0003	0.00854	85%
BBMHB 2000	20.7438	20.7437	0.0001	0.00372	90%

Table 5. Corrosion rate calculated from weight-loss data of copper in raw water and inhibition efficiency as a function of inhibitor concentration in 24 h immersion at 22° C – Batch 2.

Inhibitor Concentration (ppm)	**Initial Weight** (g)	**End Weight** (g)	**Lost Weight** (g)	**Corrosion Rate** (mmy^{-1})	**Inhibition Efficiency** (%)
Blank	20.6835	20.6823	0.0012	0.03533	-
DPLE 160	20.7382	20.7372	0.001	0.02703	23%
DPLE 320	22.772	22.7711	0.0009	0.02433	31%
DPLE 800	22.5492	22.5485	0.0007	0.02014	43%
DPLE 1000	20.2298	20.2293	0.0005	0.01430	60%
DPLE 2000	20.2291	20.2288	0.0003	0.00858	76%
BBMHB 800	23.11	23.1096	0.0004	0.01107	69%
BBMHB 1000	20.7451	20.7448	0.0003	0.00854	76%
BBMHB 2000	20.7438	20.7437	0.0001	0.00372	89%

Table 6. Corrosion rate calculated from weight-loss data of copper in raw water and inhibition efficiency as a function of inhibitor concentration in 24 h immersion at 22° C - Batch 3.

Inhibitor Concentration (ppm)	**Initial Weight** (g)	**End Weight** (g)	**Lost Weight** (g)	**Corrosion Rate** (mmy^{-1})	**Inhibition Efficiency** (%)
Blank	20.6818	20.6804	0.0014	0.03239	-
DPLE 160	20.7368	20.7356	0.0012	0.02159	21%
DPLE 320	22.7707	22.7697	0.0010	0.01889	34%
DPLE 800	22.5481	22.5475	0.0006	0.01416	58%
DPLE 1000	20.2288	20.2283	0.0005	0.00842	65%
DPLE 2000	20.2281	20.2278	0.0003	0.00595	79%
BBMHB 800	23.1091	23.1088	0.0003	0.00583	80%
BBMHB 1000	20.7446	20.7444	0.0002	0.00297	86%
BBMHB 2000	20.7432	20.7431	0.0001	0.00270	91%

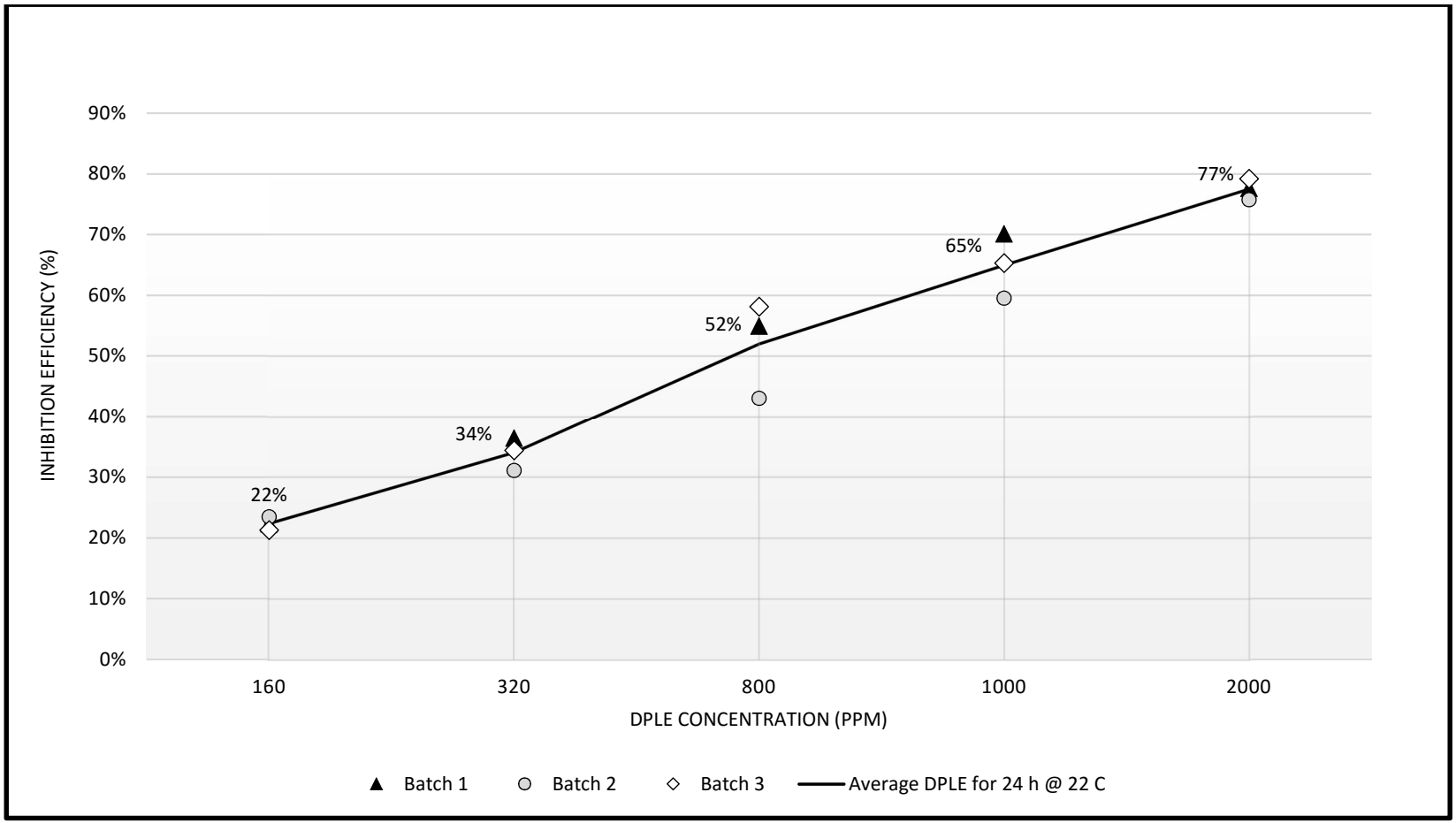

Figure 16. The average inhibition efficiency of copper in raw water vs. different concentrations of green DPLE inhibitor in 24 h immersion at 22° C for three test batches.

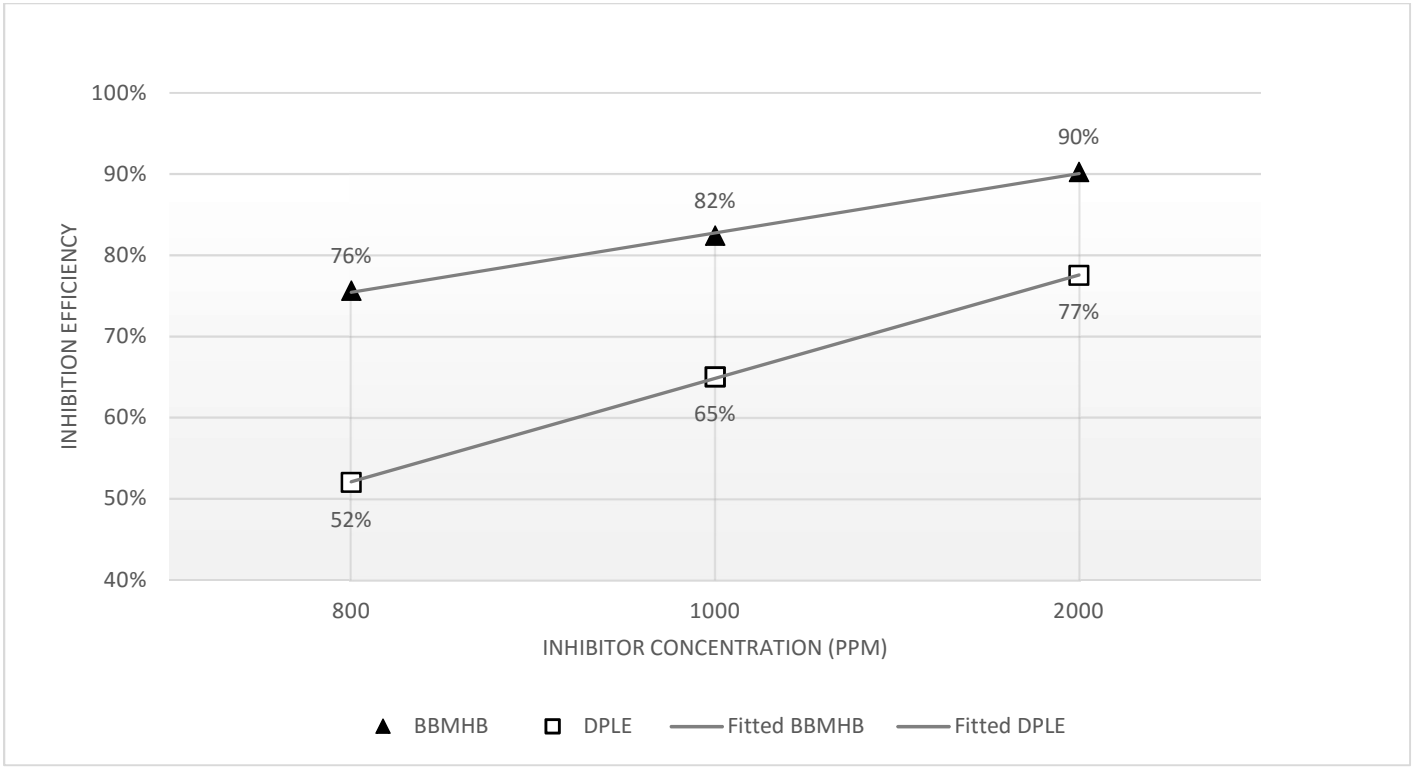

Figure 17. The average inhibition efficiency of copper in raw water vs. the concentration of green DPLE and organic BBMHB inhibitor in 24 h immersion at 22° C for three test batches.

Table 7. Corrosion rate calculated from weight-loss data of copper in raw water and inhibition efficiency as a function of inhibitor concentration in 72 h immersion at 22° C – Batch 1

Inhibitor Concentration (ppm)	**Initial Weight** (g)	**End Weight** (g)	**Lost Weight** (g)	**Corrosion Rate** (mmy^{-1})	**Inhibition Efficiency** (%)
Blank	20.6850	20.6839	0.0011	0.03839	-
DPLE 160	20.7372	20.7364	0.0008	0.02163	33%
DPLE 320	22.7735	22.7728	0.0007	0.01892	42%
DPLE 800	22.5494	22.5489	0.0005	0.01439	56%
DPLE 1000	20.2322	20.2319	0.0003	0.00858	74%
DPLE 2000	20.2316	20.2314	0.0002	0.00582	82%
BBMHB 800	23.1102	23.1100	0.0002	0.00553	83%
BBMHB 1000	20.7452	20.7451	0.0001	0.00285	91%
BBMHB 2000	20.7428	20.7427	0.0001	0.00270	92%

Table 8. Corrosion rate calculated from weight-loss data of copper in raw water and inhibition efficiency as a function of inhibitor concentration in 72 h immersion at 22° C – Batch 2.

Inhibitor Concentration (ppm)	**Initial Weight** (g)	**End Weight** (g)	**Lost Weight** (g)	**Corrosion Rate** (mmy^{-1})	**Inhibition Efficiency** (%)
Blank	20.6850	20.6839	0.0011	0.03239	
DPLE 160	20.7360	20.7352	0.0008	0.02159	33%
DPLE 320	22.7724	22.7717	0.0007	0.01889	42%
DPLE 800	22.5484	22.5479	0.0005	0.01416	56%
DPLE 1000	20.2313	20.2310	0.0003	0.00842	74%
DPLE 2000	20.2307	20.2305	0.0002	0.00595	82%
BBMHB 800	23.1095	23.1093	0.0002	0.00583	82%
BBMHB 1000	20.7444	20.7443	0.0001	0.00297	91%
BBMHB 2000	20.7415	20.7414	0.0001	0.00270	92%

Table 9. Corrosion rate calculated from weight-loss data of copper in raw water and inhibition efficiency as a function of inhibitor concentration in 72 h immersion at 22° C – Batch 3.

Inhibitor Concentration (ppm)	**Initial Weight** (g)	**End Weight** (g)	**Lost Weight** (g)	**Corrosion Rate** (mmy^{-1})	**Inhibition Efficiency** (%)
Blank	20.6843	20.6831	0.0012	0.03533	
DPLE 160	20.7358	20.7349	0.0009	0.02429	31%
DPLE 320	22.7712	22.7705	0.0007	0.01889	47%
DPLE 800	22.5482	22.5477	0.0005	0.01423	60%
DPLE 1000	20.2315	20.2312	0.0003	0.00838	76%
DPLE 2000	20.2301	20.2299	0.0002	0.00539	85%
BBMHB 800	23.1088	23.1086	0.0002	0.00553	84%
BBMHB 1000	20.7439	20.7438	0.0001	0.00285	92%
BBMHB 2000	20.7409	20.7408	0.0001	0.00270	92%

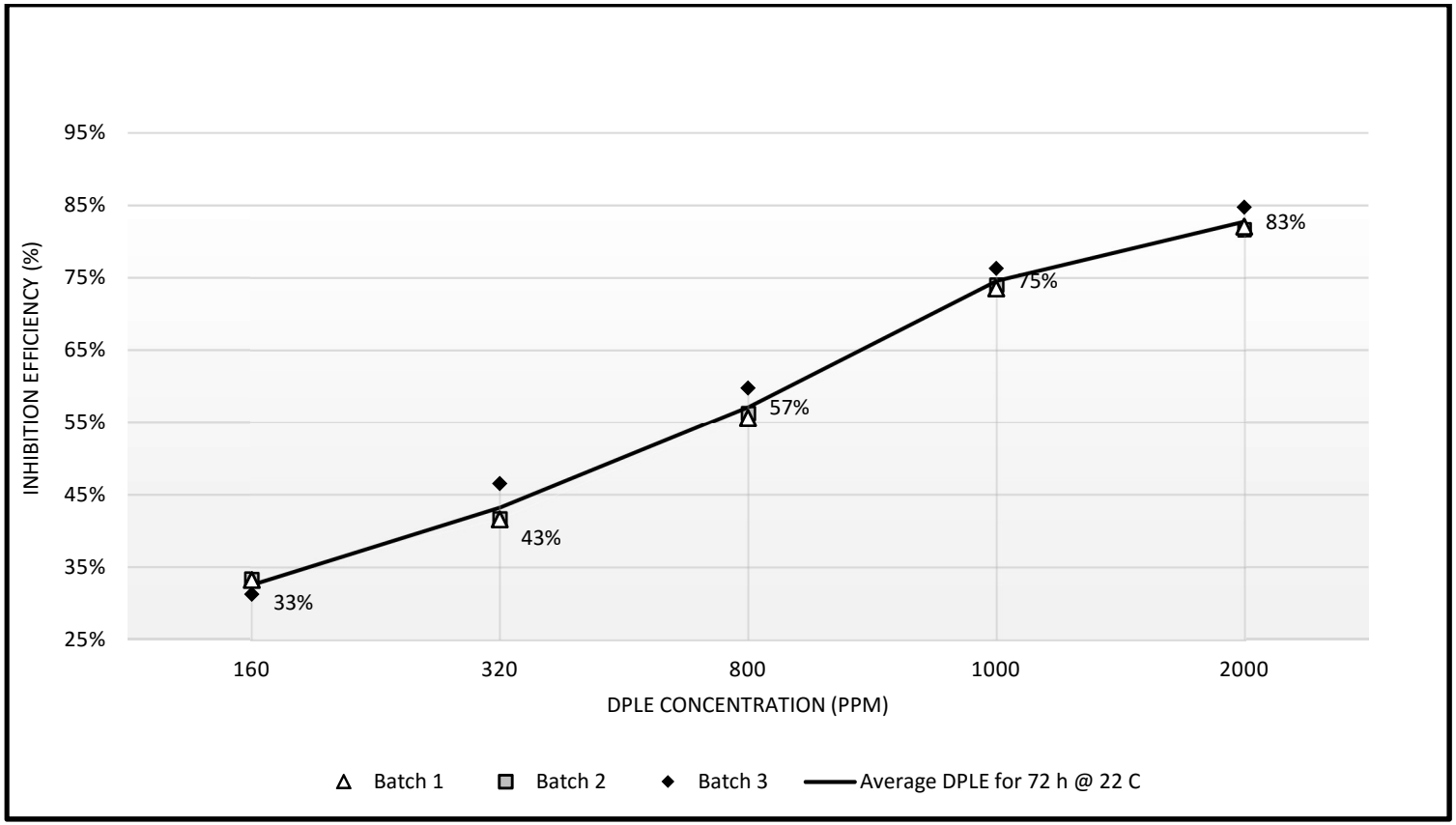

Figure 18. The average inhibition efficiency of copper in raw water vs. difference green DPLE inhibitor concentrations in 72 h immersion at 22°C for the three test batches.

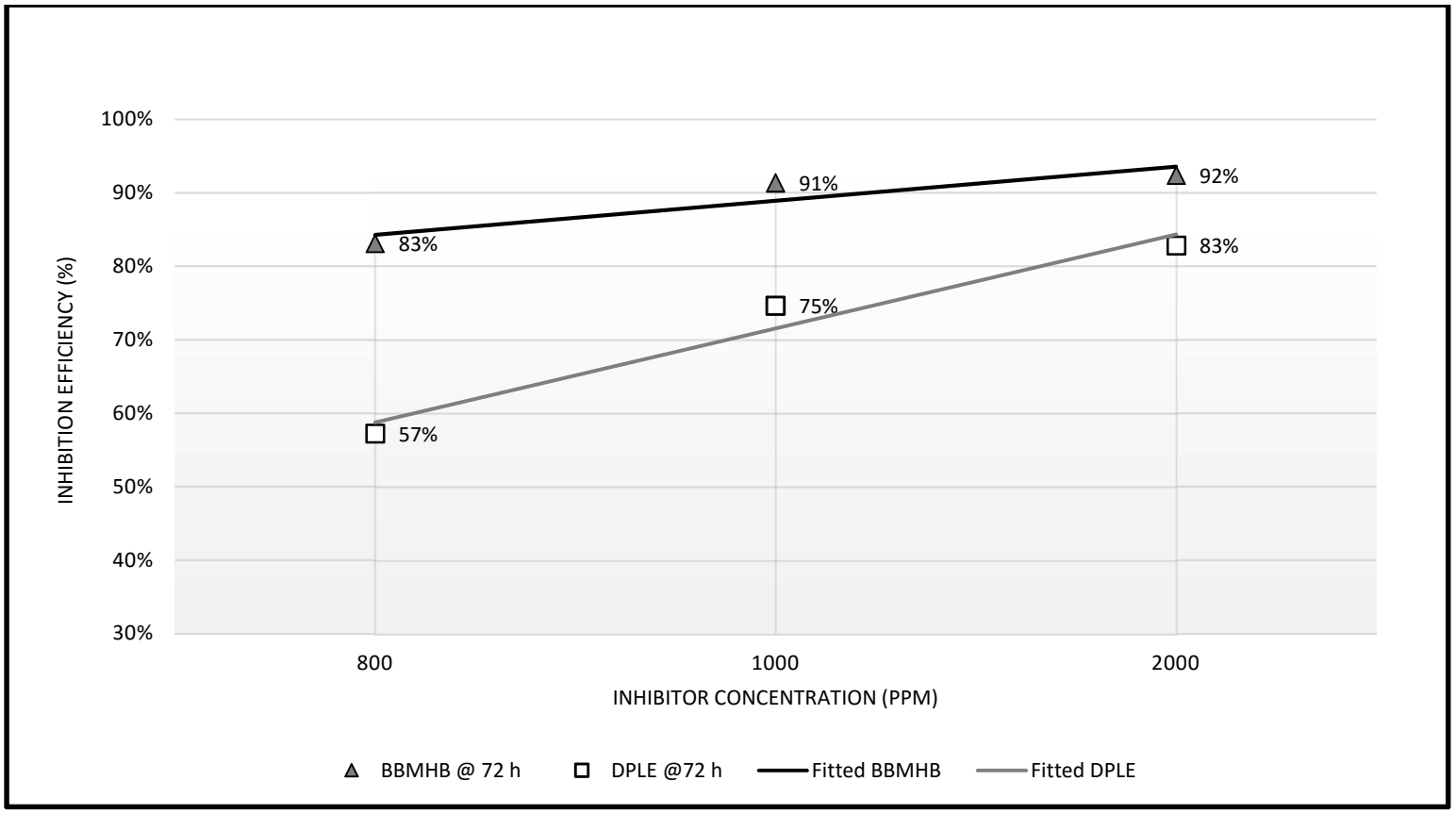

Figure 19. The average inhibition efficiency of copper in raw water vs. green DPLE and organic BBMHB inhibitor concentration in 72 h immersion at 22° C for the three test batches.

5.2 PDP Results

Figure 20 shows the potentiodynamic polarization (PDP) curves of copper in raw water, in absence and presence of DPLE and BBMHB corrosion inhibitors. Current density values decreased significantly by increasing the inhibitor concentration, hence demonstrating that both green DPLE and Organic BBMHB acted as effective corrosion inhibitors for copper in raw water media. While the inhibition efficiency of organic BBMHB was found to be higher than that of green DPLE at equal concentrations, the addition of DPLE green inhibitor reduced the corrosion rate of copper compared to uninhibited raw water. The inhibition efficiency varied proportionally with inhibitor concertation, as it did increase with increasing inhibitor concentration.

PDP data also indicated that BBMHB behaved as a mixed-type inhibitor affecting both anodic and cathodic regions of the Tafel curve. However, DPLE was clearly a cathodic inhibitor affecting the cathodic regions of Tafel curves. DPLE seems to have limited the availability of oxygen at the cathodic sites. Table 10 also shows dependence of each of corrosion potential (E_{corr}) and limiting current (I_{corr}) on the concentration of DPLE. Polarization curves for copper at different inhibitor concentrations are shown in Figure 20 and they were calculated using the following equation:

$$\text{IE } \% = \frac{(IE - IE_{blank})}{IE_{blank}} \times 100 \quad (5)$$

A significant increase in the anodic current density value can be seen in the absence of inhibitor, corresponding to the anodic dissolution of Cu, probably with the formation of Cu_2O and/or Cu(OH) film, which protects the copper substrate. Increasing the DPLE

concentration beyond 2000 ppm produces a plateau in efficiency, which did not increase much between 2000 and 3000 ppm. Hence, the optimum concentration of DPLE seems to be around 2000 ppm for inhibiting copper in raw water solutions. The cathodic reaction should be the reduction of water,

$$2H_2O + 2e^- = H_2 + 2OH^- \quad (6)$$

The presence of oxygen enhances the cathodic reaction due to oxygen reduction, and/or the water reduction [42].

$$O_2 + 2H_2O + 4e^- = 4OH^- \quad (7)$$

This causes copper to corrode rapidly to form a porous oxide film,

$$2Cu + H_2O = Cu_2O + 2H^+ + 2e^- \quad (8)$$

which is in good electrical contact with the underlying metal. At this condition, the anodic dissolution of copper without inhibitor occurs through oxidation of $Cu(_0)$ to Cu^+. This is due to the presence of oxygen in the solution might have led to formation of an oxide film on the copper surface at this potential,

$$Cu = Cu^+ + e^- \quad (9)$$

$$2Cu + 0.5\ O_2 = Cu_2O \quad (10)$$

Table 10. Corrosion potential, the corrosion current from Tafel polarization curves of copper in raw water and inhibition efficiency as a function of inhibitor concentration at 22° C

Inhibitor Concentration (ppm)	**β_a** (V/decade) $\times 10^{-2}$	**β_c** (V/decade) $\times 10^{-2}$	**I_{corr}** (nA cm^{-2})	**E_{corr}** (mV)	**Corrosion Rate** (mmy^{-1})	**Inhibition Efficiency** (%)
Blank	6.18	9.75	1310	-105	0.01926	-
DPLE 160	5.13	4.71	657	-114	0.00966	50 %
DPLE 320	3.88	2.86	522	-92.1	0.00768	60%
DPLE 800	4.40	6.25	323	-123	0.00475	75%
DPLE 2000	2.80	2.85	147	-155	0.00129	93%
DPLE 3000	9.03	5.20	129	-113	0.00114	94%
BBMHB 800	4.14	4.18	128	-94.4	0.00189	90%

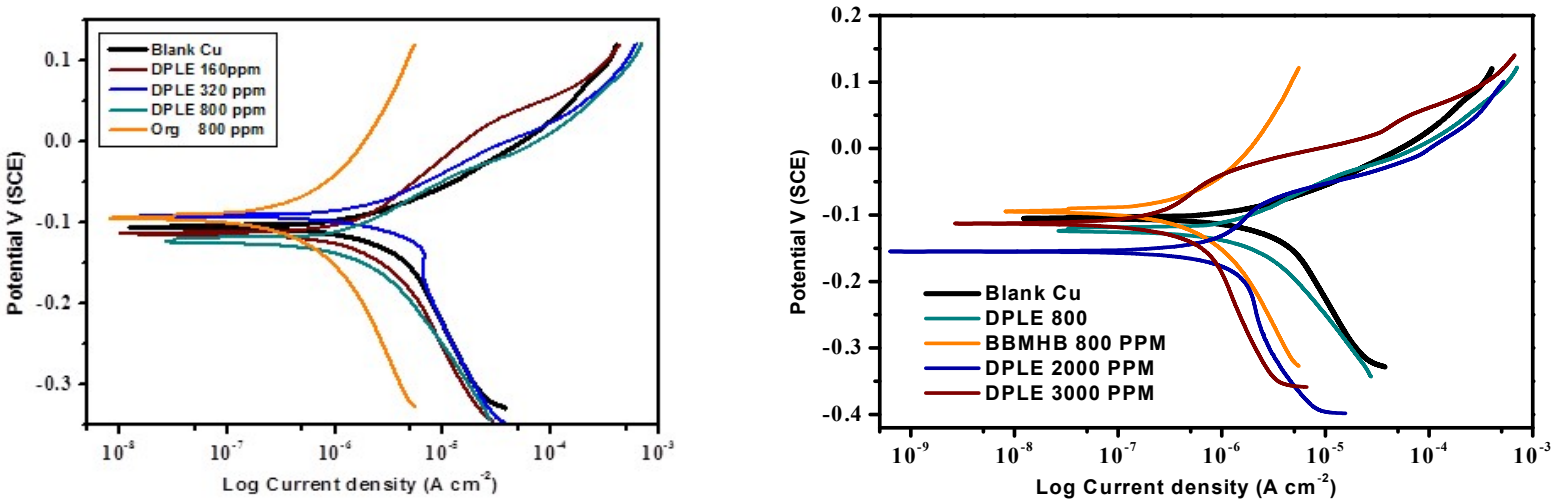

a) b)

Figure 20. Potentiodynamic polarization (PDP) curves of copper in raw water, in absence and presence of DPLE and BBMHB at 22° C (a and b).

5.3 EIS Results

Impedance experiments were conducted to gain insight into the characteristics and kinetics of electrochemical processes occurring at the Cu/raw water interface in the absence and presence of inhibitor. The impedance spectra of Nyquist plots for copper in raw water in absence of inhibitor were analyzed by fitting the experimental data to the Randles equivalent circuit model shown in Figure 21. In this circuit, R_s represents the solution resistance, R_{ct} is the charge transfer resistance and C_{dl} is the double layer capacitance.

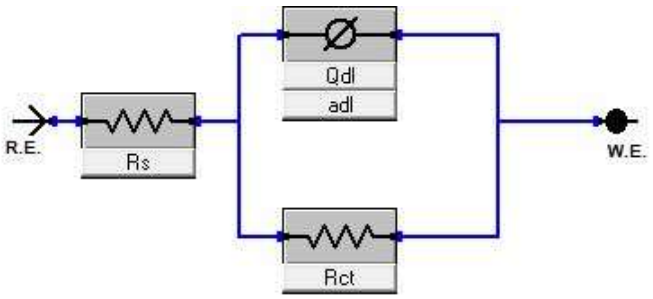

Figure 21. Equivalent circuit diagram used to fit impedance data of copper in raw uninhibited water.

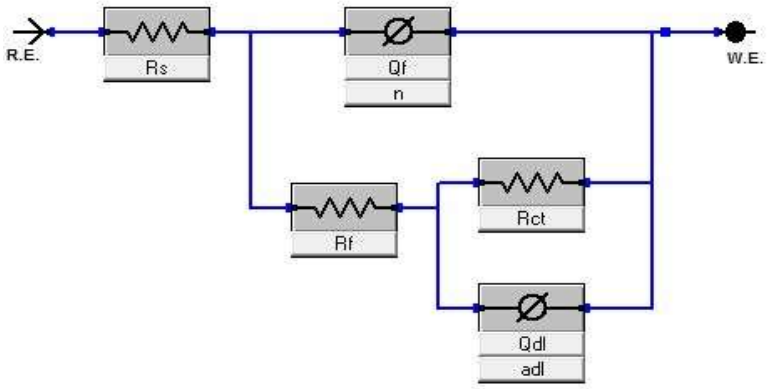

Figure 22. Equivalent circuit diagram used to fit impedance data of copper in raw water in the presence of DPLE and BBMHB.

Figure 22 shows the equivalent circuit diagram used to fit the impedance data of copper in raw water in the presence of inhibitor. This is similar to Randles equivalent circuit with the addition of R_f being the charge transfer resistance across inhibitor adsorbed film on the copper surface, and Q_f being the capacitance across that same film. The influence of DPLE and BBMHB corrosion inhibitors' concentration on the impedance spectra of copper electrode in aerated raw water at room temperature is depicted in Figures 23 and 24. In all cases, the Nyquist plots are not perfect semicircles. This phenomenon is related to the roughness and in-homogeneity of the electrode surface. The semicircle corresponds to a capacitive loop. The semicircle radii depend on the concentration of the DPLE. The diameter of the capacitive loop increases with increasing the concentration of green DPLE. The values of charge transfer resistance (R_{ct}) and double layer capacitance (C_{dl}) were obtained using the Nyquist plots and are given in Table 11.

To obtain the double layer capacitance C_{dl}, the frequency (F_{max}) at which the imaginary component of the impedance is maximum was found and C_{dl} values were obtained from the equation:

$$C_{dl} = \frac{1}{2\pi F_{max} R_{ct}} \tag{11}$$

Charge transfer resistance is correlated to the corrosion current density for relatively simple corrosion systems characterized by a charge transfer controlled process. The inhibition efficiency ($\eta_R\%$) was calculated using the following equation:

$$\eta\% = \frac{(R_{ct} - R_{blank})}{R_{blank}} \times 100 \tag{12}$$

where R_{ct} and R_{blank} are the charge transfer resistance with and without inhibitor, respectively. The values of inhibition efficiency are listed in Table 11. It was noticed from Table 11 that the increasing concentration of DPLE caused increase in the charge transfer resistance R_{ct} and this, in turn, leads to an increase in inhibition efficiency $\eta_R\%$. As seen from Table 11, the presence of DPLE leads to the decrease in C_{dl} values. The decrease in C_{dl} values was caused by adsorption of DPLE and BBMHB inhibitors to the surface of the copper substrate. Moreover, the data clearly showed that when DPLE concentration increased, C_{dl} decreased. This behavior may be result from a decrease in local dielectric constant and/or an increase in the thickness of the electrical double layer, which suggests that the DPLE might be driven by adsorption at the metal-solution interface.

Figures 23 and 24 show Bode resistance and phase angle plots, respectively - where the real and imaginary impedance components were plotted over the frequency range of 100 kHz to 100 MHz, for the copper electrode in raw water solutions with and without DPLE and BBMHB inhibitors at ambient temperature. The Bode plots in Figure 23 showed high impedance in the low frequency region in the presence of DPLE, which suggests the formation of an inhibitor film responsible for this high resistance. The impedance at higher frequency was low and corresponds to the impedance of the solution.

The Nyquist plots in Figure 25 obtained in the presence of DPLE show a small semi-circle in the high frequency region, a large semi-circle, which represents the polarization resistance (R_f).

Table 11. Electrochemical impedance parameters of copper corrosion in raw water, and inhibition efficiency as a function of inhibitor concentration at 22° C.

Inhibitor Concentration (ppm)	**R_s** (Ω cm^2)	**R_{ct} (× 10^{-3})** (Ω cm^2)	**C_{dl} (× 10^{6})** (μ F cm^{-2})	**n_1**	**R_f** (μ F cm^{-2})	**Q_f (× 10^{6})** (μ F cm^{-2})	**n_2**	**Inhibition Efficiency η_R** (%)
Blank	176.00	3.45	165.00	0.581	0	0	0	-------
DPLE 160	151.20	3.74	106.00	0.270	509.4	9.92	0.86	8%
DPLE 320	143.10	4.71	73.80	0.532	123.2	12.34	0.91	27%
DPLE 800	113.80	9.16	33.46	0.350	726.7	4.98	0.90	62%
BBMHB 800	150.60	31.93	12.19	0.588	1050.0	2.46	0.81	89%

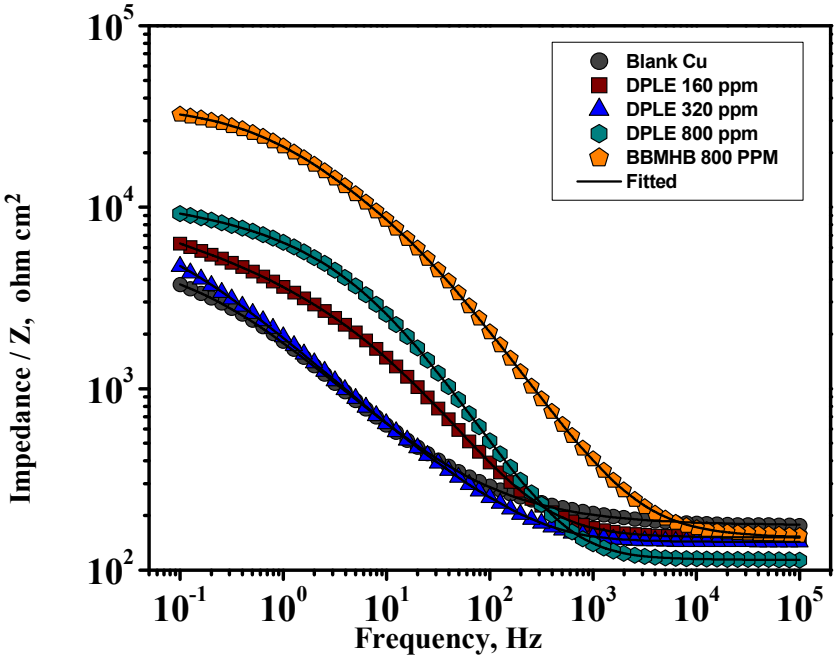

Figure 23. Bode Resistance Plot curves of copper in raw water, in absence and presence of green DPLE and organic BBMHB at 22˚ C.

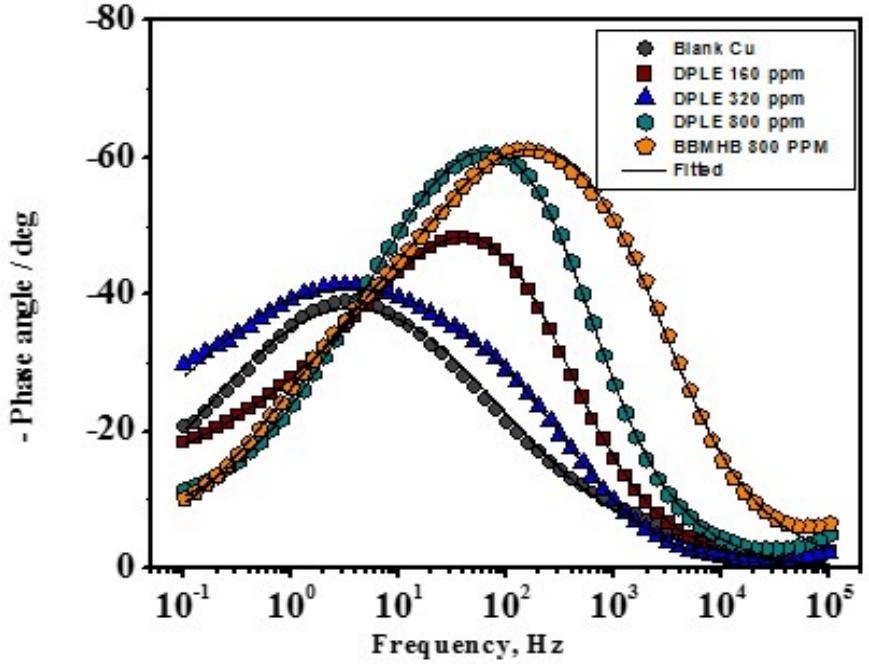

Figure 24. Bode Phase Plot curves of copper in raw water, in absence and presence of green DPLE and organic BBMHB at 22˚ C.

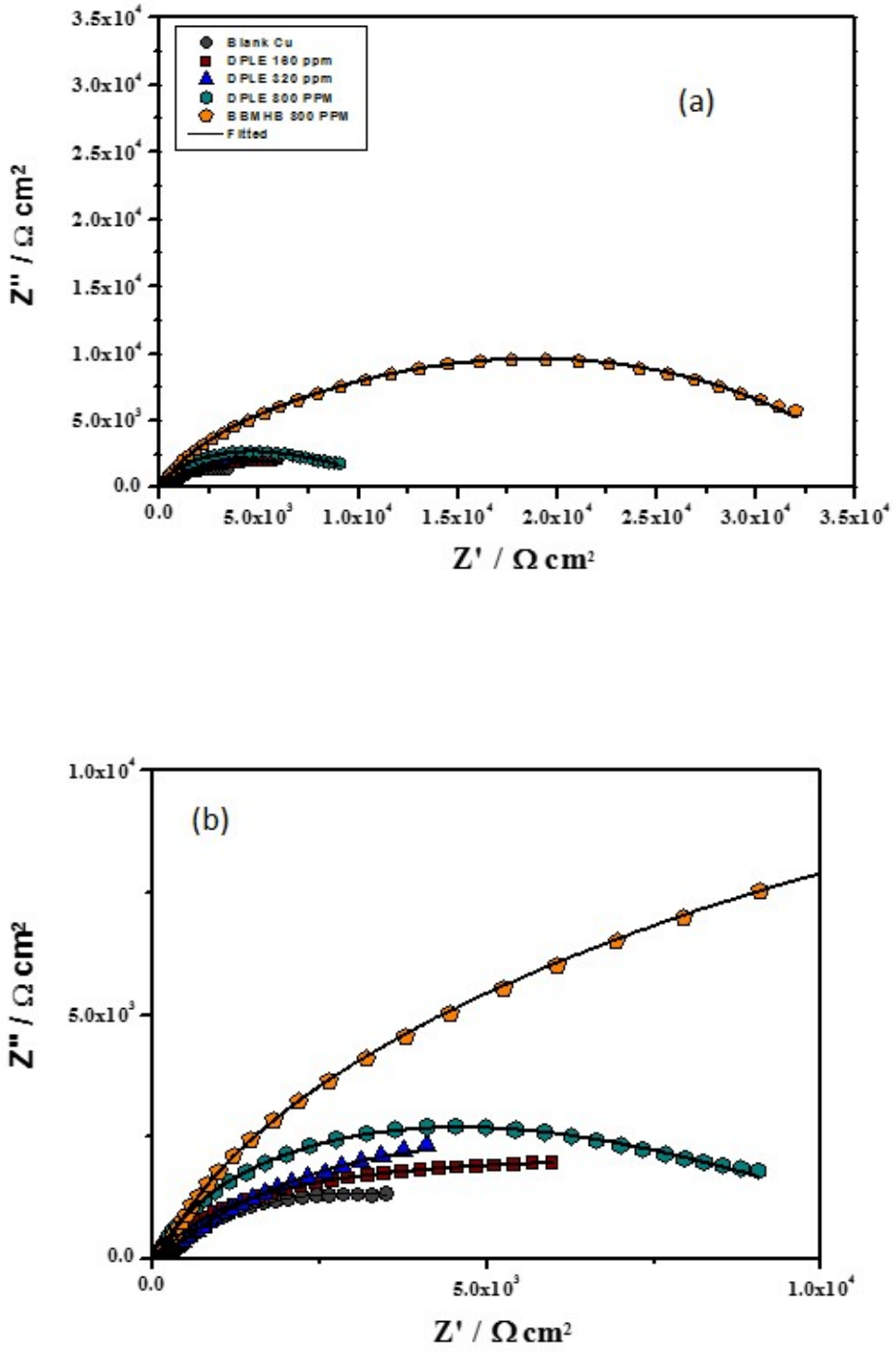

Figure 25. Nyquist Phase Plot curves (a) of copper in raw water, in absence and presence of green DPLE and organic BBMHB at 22° C and (b) is the expanded portion of (a).

5.4 The Effect of Temperature:

In order to evaluate the effect of the temperature on the corrosion inhibition effect of green DPLE corrosion inhibitor, the weight loss experiments were undertaken at 22, 40 and 60°C for 24 h immersion time. Tables 4, 5 and 6 in section 5.1 showed the weight loss data collected after 24 h immersion test samples in raw water at 22° C. Tables 12 to 17 show the weight loss data collected after 24 h immersion test samples in raw water at 40° and 60° C. Each concentration was tested 3 times in order to validate the collected weight loss data. The average inhibition efficiency from these tables was then plotted in Figures 27 and 26.

The obtained results showed that corrosion rates increased with an increase in the temperature in the absence and presence of green DPLE and organic BBMHB corrosion inhibitors. A decrease in the inhibition efficiency with increasing temperature is often attributed to desorption of inhibitor molecules from metal surface [37]. The desorption process is enhanced by increasing the temperature of the solution, which increases the system overall energy, hence promoting dispersal of the adsorbed inhibitor from the metal surface. Accordingly, an increase in the temperature is accompanied by desorption of those constituents of green DPLE and organic BBMHB that are adsorbed to the metal surface, leading to reduced surface coverage and, hence, lower inhibition efficiency. Nevertheless, results showed that green DPLE still recorded good inhibition efficiency at high temperatures compared to uninhibited raw water.

Table 12. Corrosion rate calculated by weight-loss method of copper in raw water and inhibition efficiency as a function of inhibitor concentration in 24 h immersion at 40° C – Batch 1.

Inhibitor Concentration	**Initial Weight**	**End Weight**	**Lost Weight**	**Corrosion Rate**	**Inhibition Efficiency @ 40° C**
(ppm)	(g)	(g)	(g)	(mmy^{-1})	(%)
Blank	20.6831	20.6820	0.0011	0.0327	-
DPLE 160	20.7349	20.7339	0.0010	0.0270	17%
DPLE 320	22.7705	22.7696	0.0009	0.0243	26%
DPLE 800	22.5477	22.5470	0.0007	0.0199	39%
DPLE 1000	20.2312	20.2307	0.0005	0.0140	57%
DPLE 2000	20.2299	20.2296	0.0003	0.0081	75%
BBMHB 800	23.1086	23.1080	0.0006	0.0166	49%
BBMHB 1000	20.7438	20.7433	0.0005	0.0142	56%
BBMHB 2000	20.7408	20.7405	0.0003	0.0081	75%

Table 13. Corrosion rate calculated by weight-loss method of copper in raw water and inhibition efficiency as a function of inhibitor concentration in 24 h immersion at 40° C – Batch 2.

Inhibitor Concentration	**Initial Weight**	**End Weight**	**Lost Weight**	**Corrosion Rate**	**Inhibition Efficiency @ 40 ° C**
(ppm)	(g)	(g)	(g)	(mmy^{-1})	(%)
Blank	20.6815	20.6801	0.0014	0.0416	-
DPLE 160	20.7333	20.7320	0.0013	0.0351	16%
DPLE 320	22.7691	22.7679	0.0012	0.0324	22%
DPLE 800	22.5466	22.5457	0.0009	0.0256	38%
DPLE 1000	20.2300	20.2292	0.0008	0.0223	46%
DPLE 2000	20.2288	20.2283	0.0005	0.0135	68%
BBMHB 800	23.1076	23.1069	0.0007	0.0194	53%
BBMHB 1000	20.7429	20.7423	0.0006	0.0171	59%
BBMHB 2000	20.7400	20.7397	0.0003	0.0081	81%

Table 14. Corrosion rate calculated by weight-loss method of copper in raw water and inhibition efficiency as a function of inhibitor concentration in 24 h immersion at 40° C – Batch 3.

Inhibitor Concentration	**Initial Weight**	**End Weight**	**Lost Weight**	**Corrosion Rate**	**Inhibition Efficiency @ 40 ° C**
(ppm)	(g)	(g)	(g)	(mmy^{-1})	(%)
Blank	20.6794	20.6774	0.0020	0.0595	-
DPLE 160	20.7316	20.7297	0.0019	0.0514	14%
DPLE 320	22.7673	22.7656	0.0017	0.0459	23%
DPLE 800	22.5453	22.5439	0.0014	0.0398	33%
DPLE 1000	20.2285	20.2272	0.0013	0.0363	39%
DPLE 2000	20.2277	20.2269	0.0008	0.0216	64%
BBMHB 800	23.1065	23.1056	0.0009	0.0249	58%
BBMHB 1000	20.7417	20.7409	0.0008	0.0228	62%
BBMHB 2000	20.7391	20.7387	0.0004	0.0108	82%

Table 15. Corrosion rate calculated by weight-loss method of copper in raw water and inhibition efficiency as a function of inhibitor concentration in 24 h immersion at 60° C – Batch 1.

Inhibitor Concentration	**Initial Weight**	**End Weight**	**Lost Weight**	**Corrosion Rate**	**Inhibition Efficiency @ 60 ° C**
(ppm)	(g)	(g)	(g)	(mmy^{-1})	(%)
Blank	20.6779	20.6764	0.0015	0.0446	-
DPLE 160	20.7301	20.7286	0.0015	0.0406	9%
DPLE 320	22.7662	22.7648	0.0014	0.0378	15%
DPLE 800	22.5442	22.5431	0.0011	0.0313	30%
DPLE 1000	20.2276	20.2266	0.0010	0.0279	37%
DPLE 2000	20.2273	20.2266	0.0007	0.0189	58%
BBMHB 800	23.1062	23.1053	0.0009	0.0249	44%
BBMHB 1000	20.7413	20.7405	0.0008	0.0228	49%
BBMHB 2000	20.7391	20.7384	0.0007	0.0189	58%

Table 16. Corrosion rate calculated by weight-loss method of copper in raw water and inhibition efficiency as a function of inhibitor concentration in 24 h immersion at 60° C – Batch 2.

Inhibitor Concentration	**Initial Weight**	**End Weight**	**Lost Weight**	**Corrosion Rate**	**Inhibition Efficiency @ 60° C**
(ppm)	(g)	(g)	(g)	(mmy^{-1})	(%)
Blank	20.6759	20.6745	0.0014	0.0416	-
DPLE 160	20.7281	20.7267	0.0014	0.0379	9%
DPLE 320	22.7643	22.7630	0.0013	0.0351	16%
DPLE 800	22.5426	22.5417	0.0009	0.0256	38%
DPLE 1000	20.2261	20.2252	0.0009	0.0251	40%
DPLE 2000	20.2261	20.2254	0.0007	0.0189	55%
BBMHB 800	23.1048	23.1040	0.0008	0.0221	47%
BBMHB 1000	20.7400	20.7393	0.0007	0.0199	52%
BBMHB 2000	20.7379	20.7373	0.0006	0.0162	61%

Table 17. Corrosion rate calculated by weight-loss method of copper in raw water and inhibition efficiency as a function of inhibitor concentration in 24 h immersion at 60° C – Batch 3.

Inhibitor Concentration	**Initial Weight**	**End Weight**	**Lost Weight**	**Corrosion Rate**	**Inhibition Efficiency @ 60° C**
(ppm)	(g)	(g)	(g)	(mmy^{-1})	(%)
Blank	20.6740	20.6720	0.0020	0.0595	-
DPLE 160	20.7261	20.7241	0.0020	0.0541	9%
DPLE 320	22.7624	22.7605	0.0019	0.0513	14%
DPLE 800	22.5411	22.5397	0.0014	0.0398	33%
DPLE 1000	20.2246	20.2233	0.0013	0.0363	39%
DPLE 2000	20.2247	20.2238	0.0009	0.0243	59%
BBMHB 800	23.1034	23.1023	0.0011	0.0304	49%
BBMHB 1000	20.7386	20.7376	0.0010	0.0285	52%
BBMHB 2000	20.7366	20.7357	0.0009	0.0243	59%

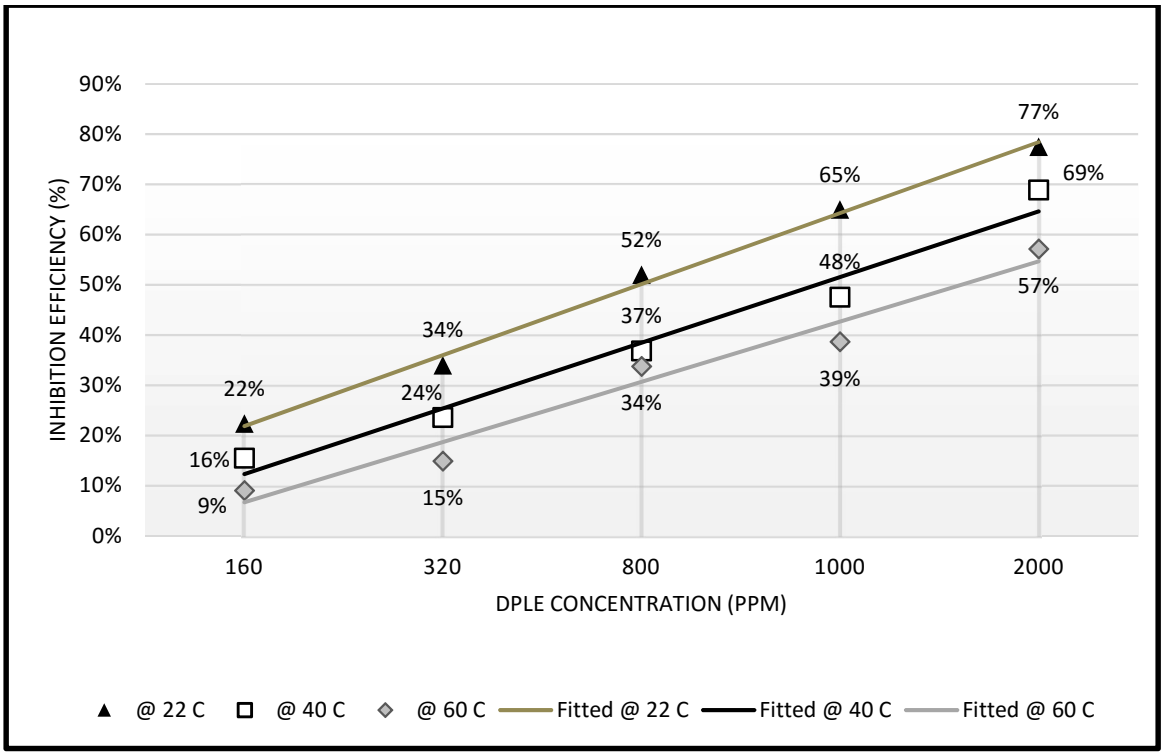

Figure 26. The Effect of temperature on the average inhibition efficiency at different concentrations of green DPLE inhibitor in 24 h Immersion at 22, 40 and 60˚ C for the three test batches.

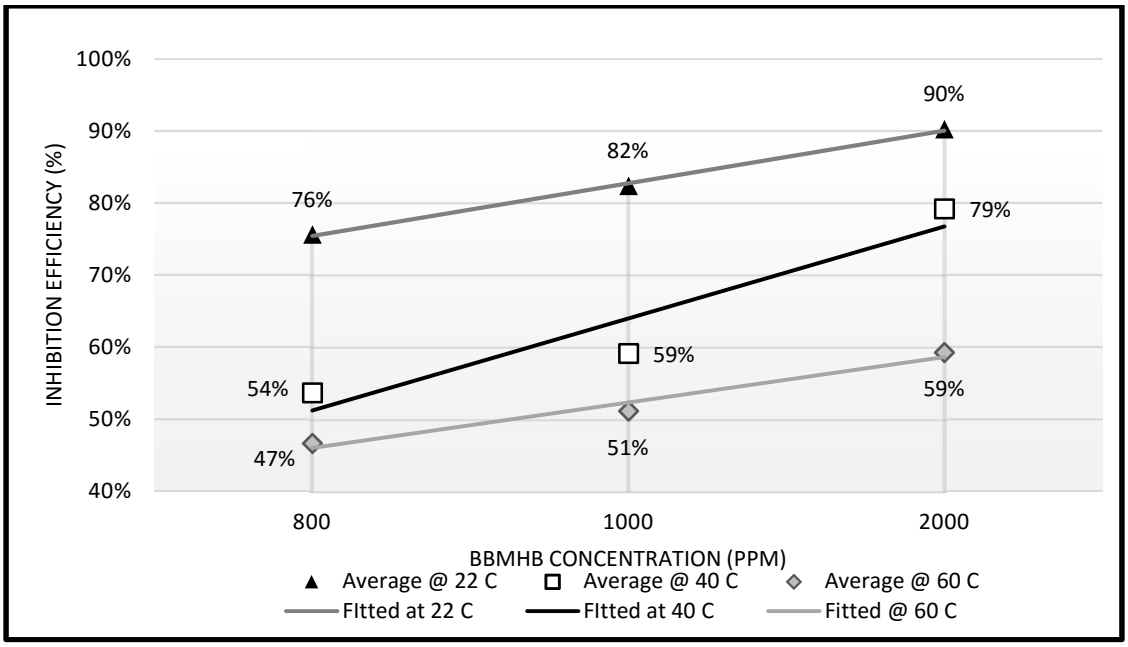

Figure 27. The Effect of temperature on the average inhibition efficiency at different concentrations of BBMHB organic inhibitor in 24 h Immersion at 22, 40 and 60º C for the three test batches.

5.5 The Effect of Time

In order to evaluate the effect of the exposure time on the corrosion inhibition effect of green DPLE corrosion inhibitor, the weight loss experiments were undertaken at 22°C for 24 and 72 h immersion periods. The results obtained are listed in Table 18 and are plotted in Figure 28, which show that corrosion rates increased with an increase in immersion time in the absence and presence of green DPLE. The inhibition efficiency of green DPLE corrosion inhibitor increased with a longer immersion period. An increase in the inhibition efficiency with increasing immersion time can be attributed to extended adsorption of inhibitor species on the corroding metal surface, and the stable film resulting from this adsorption. Adsorption process is enhanced by increasing the immersion time. Accordingly, the inhibition efficiency of green DPLE inhibitor was found to increase with immersion time as green DPLE inhibitor continues to be adsorbed to the metal surface, leading to increased surface coverage and, hence, higher corrosion efficiency. The same can similarly be said about the organic BBMHB inhibitor. Figure 29 shows a comparative analysis between the behavior of green DPLE and organic BBMHB as both corrosion inhibitors performed comparably well at similar concentrations, with the organic BBMHB showing a slight improvement over its green DPLE counterpart.

Table 18.The Effect of Time on the corrosion rate calculated by weight-loss method of copper in raw water and inhibition efficiency as a function of inhibitor concentration in 24 and 72 h immersion at 22°C.

	24 h		**72 h**	
Inhibitor Concentration (ppm)	Corrosion Rate (mmy^{-1})	Average Inhibition Efficiency (%)	Corrosion Rate (mmy^{-1})	Average Inhibition Efficiency (%)
Blank	0.0363	-	0.0334	-
DPLE 160	0.0270	22%	0.0225	33%
DPLE 320	0.0225	34%	0.0189	43%
DPLE 800	0.0172	52%	0.0143	57%
DPLE 1000	0.0114	65%	0.0085	75%
DPLE 2000	0.0075	77%	0.0057	83%
BBMHB 800	0.0083	76%	0.0056	83%
BBMHB 1000	0.0057	82%	0.0029	91%
BBMHB 2000	0.0034	90%	0.0027	92%

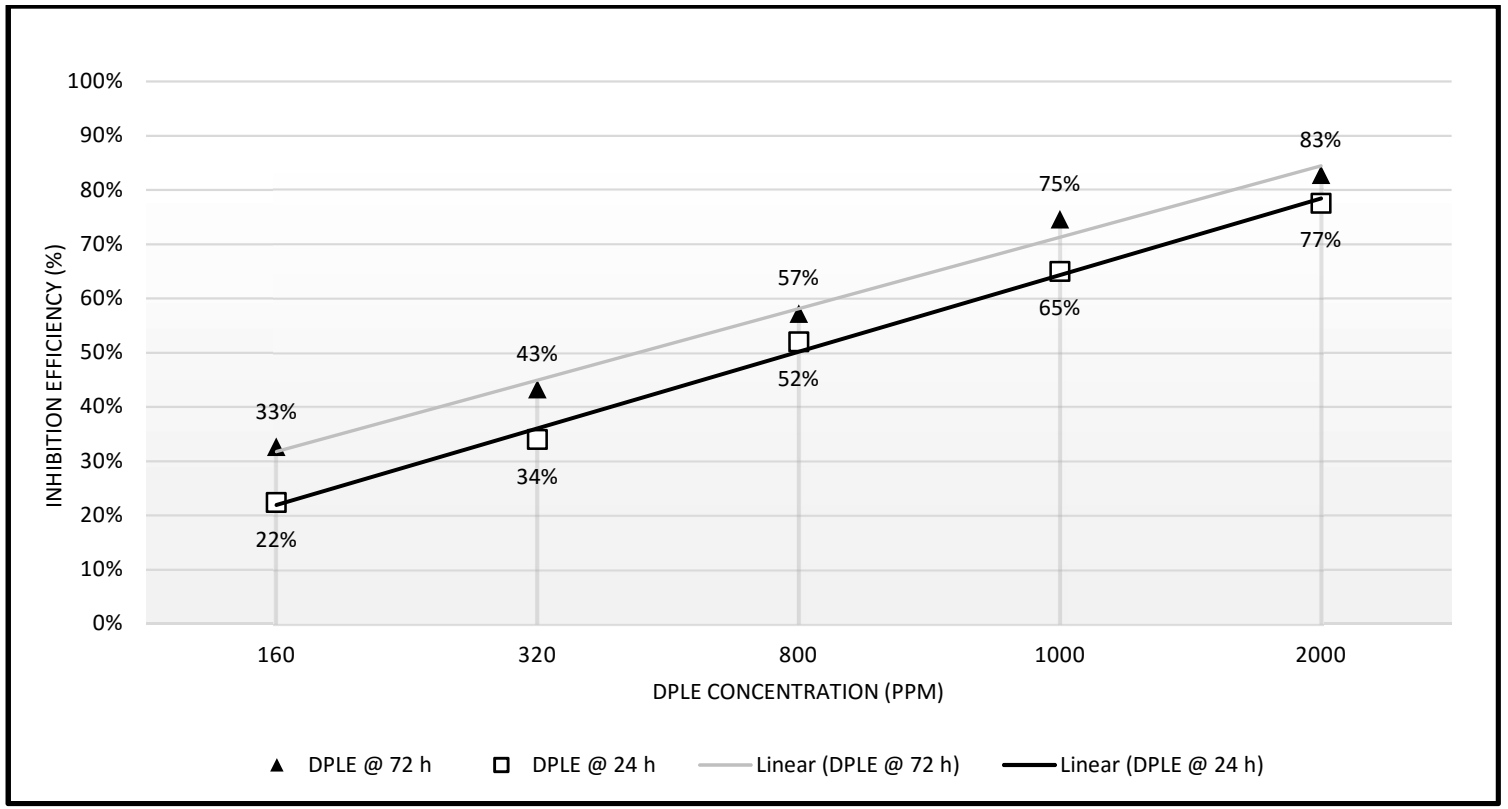

Figure 28. Effect of Time on the inhibition efficiency of DPLE of copper in raw water with different concentrations of green DPLE inhibitor at 22˚C.

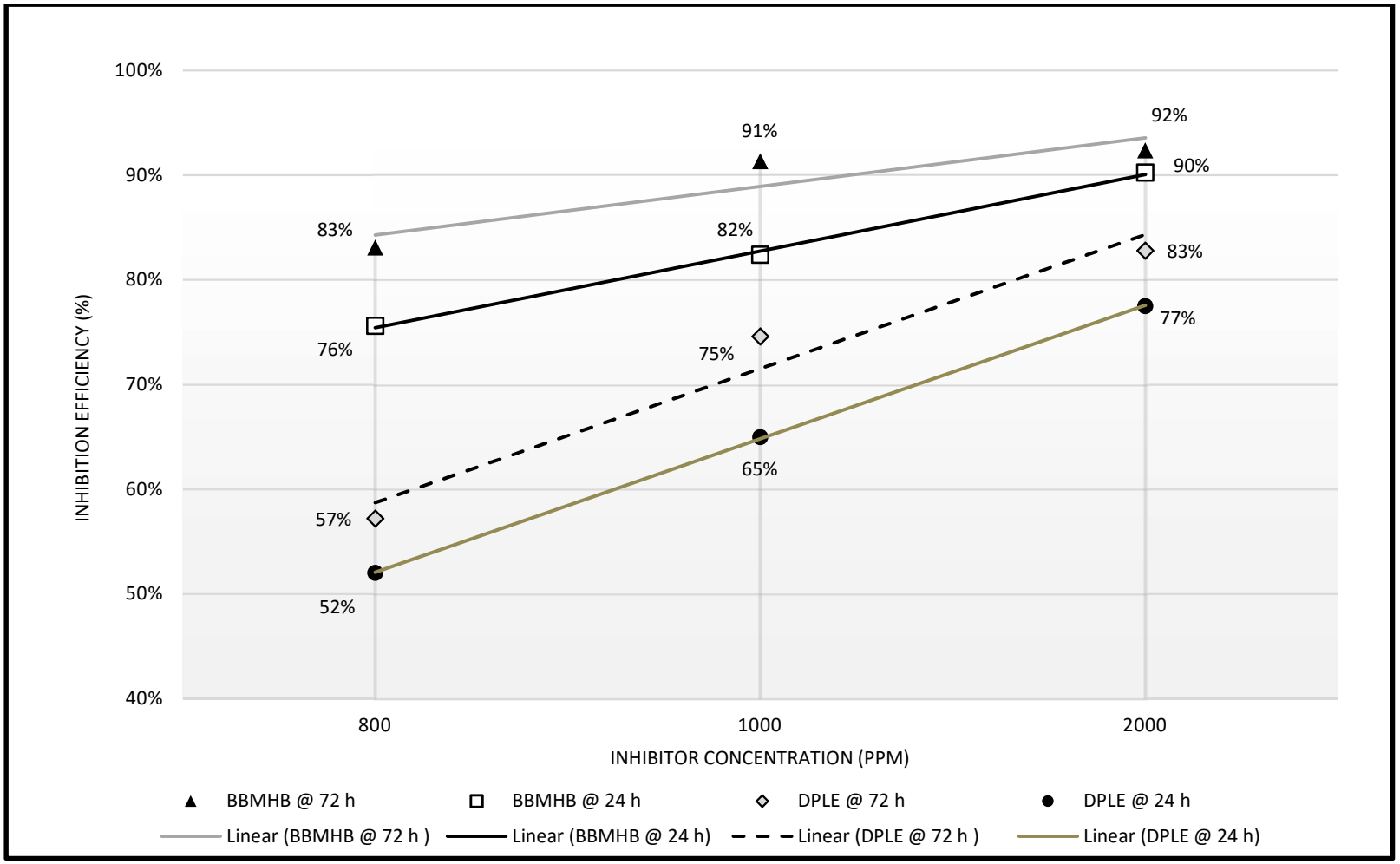

Figure 29. The Effect of Time on the corrosion rate calculated by weight-loss method of copper in raw water and inhibition efficiency as a function of inhibitor concentration in 24 and 72 h immersion at 22° C.

5.6 Adsorption Isotherms

Organic inhibitors are believed to inhibit metal corrosion by an adsorption mechanism whereby the inhibitor molecules gradually substitute the adsorbed water molecules on the metal surface [45] [47] [48]. Two types of adsorption are defined in the literature: physisorption and chemisorption [49] [50]. Physisorption has to do with the electrostatic interaction between charged inhibitor molecules and a charged metal, while chemisorption involves charge sharing or transfer from the inhibitor components to a metal surface to form a coordinate type of bond [50]. Interestingly, these two types of adsorption can occur on the same surface. Certain factors such as the chemical composition of the inhibitor molecule, concentration of both the inhibitor and corrosive solution, electronic properties of the inhibitor molecule and the temperature of the aggressive medium [49] have an influence on the type of adsorption that prevails over the other in a metal surface. Theoretically, low temperatures favor physical adsorption because of the low heat of adsorption, while elevated temperatures favor chemical adsorption owing to its stronger adsorption energy compared to physisorption [49]. Basic information regarding the predominant adsorption mechanism can be obtained using a suitable adsorption isotherm [49].

The results have shown that the inhibition efficiency is directly dependent on the concentration of inhibitor. The efficiency of an inhibitor depends on its ability to occupy the respective vacant sites forming a chemisorbed inhibitor film. This efficiency also depends on the composition of the metal, inhibitor structure and concentration as well as temperature. The adsorption process is often studied graphically using adsorption

isotherms. These models provide information on the interaction between adsorbed species at the metal/electrolyte interface.

$$\text{Adsorbate} + \text{Adsorbent} \underset{\text{desorption}}{\overset{\text{Adsorption}}{\rightleftharpoons}} \text{Adsorption}$$

$$A + B \rightleftharpoons AB \tag{13}$$

In the process of adsorption, adsorbate gets adsorbed on adsorbent. According to Le-Chatelier principle, the direction of equilibrium would shift in that direction where the stress can be relieved. In case of application of excess of pressure to the equilibrium system, the equilibrium will shift in the direction where the number of molecules decreases. Since number of molecules decreases in forward direction, with the increases in pressure, forward direction of equilibrium will be favored.

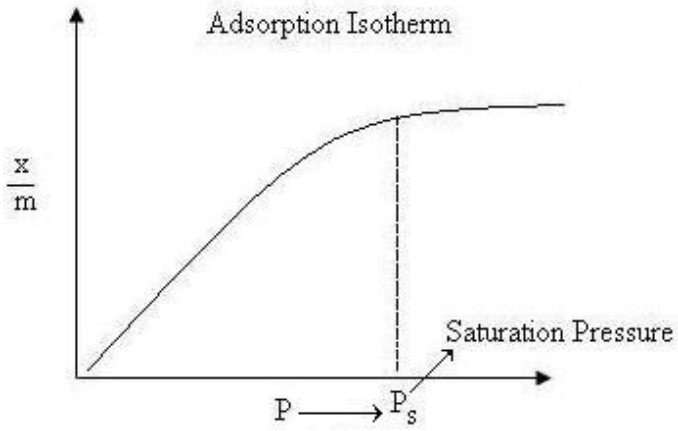

Figure 30. Basic Adsorption Isotherm.

From Figure 30, we can predict that after saturation pressure Ps, adsorption does not occur anymore. This can be explained by the fact that there are limited numbers of vacancies on

the surface of the adsorbent. At high pressure a stage is reached when all the sites are occupied and further increase in pressure does not cause any difference in adsorption process. At high pressure, Adsorption is independent of pressure.

The magnitude of surface coverage (θ) from EIS measurements obtained using equation 14 (assuming a direct relation between surface coverage (θ) and inhibition efficiency (IE%) was employed for a particular range of inhibitor concentrations:

$$IE\% = \theta \times 100 \quad (14)$$

By fitting the experimentally derived surface coverage values (obtained from Eq. 14) at different concentrations, the model will be adopted that best matches the data by virtue of evaluating the closeness of values of the slope to unity in comparison to Equation 15. In this study, linear experimental data in Figure 31 shows that adsorption of the constituents of DPLE onto a copper surface followed the Langmuir adsorption isotherm model (mathematically expressed in Equation 15). The Langmuir adsorption isotherm postulates the inhibitor adsorption as a monolayer, as well as the independency in molecular adsorption with the number of available sites:

$$C/\Theta = C + 1/K_{ads} \quad (15)$$

K_{ads} = *Equilibrium constant associated with the interfacial molecular adsorption*

C = *Inhibitor concentration (measured in ppm)*

θ = *Magnitude of the surface coverage of individual inhibitors on the* copper

The Langmuir plot, as C/θ vs. C, is shown to be linear in Figure 31, indicating that molecular adsorption of green DPLE and organic BBMHB inhibitors on the surface of the copper substrate within the range of concentrations of the inhibitors studied at 22°C could be approximated by this adsorption isotherm model. The equations of the two fitted lines for DPLE and BBMHB have unity slopes similar to that of equation (15), confirming that both green DPLE and organic BBMHB corrosion inhibitors conformed to the Langmuir adsorption isotherm.

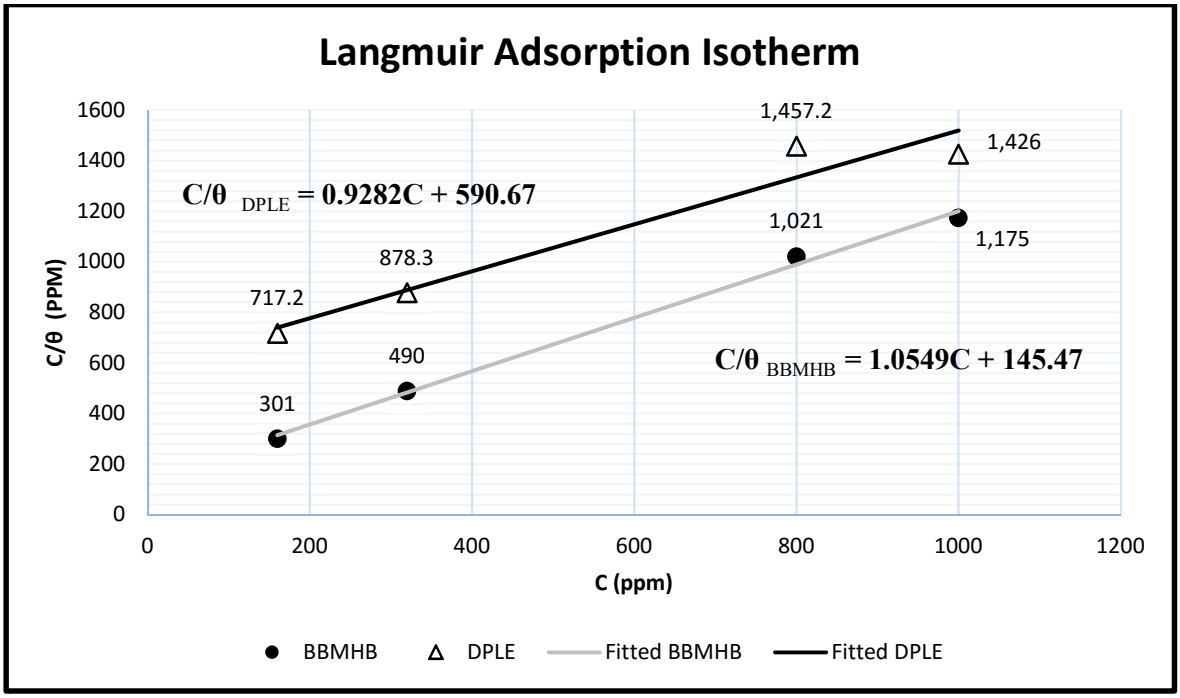

Figure 31. Langmuir adsorption isotherm for DPLE and BBMHB on copper corrosion in raw water obtained from EIS measurements.

5.7 FT-IR Spectroscopy Results

Analysis of FT-IR spectra was used to analyze the protective film that had formed on the copper metal surface. FT-IR spectrum analysis of corroded copper sample in DPLE inhibited raw water is shown in Figure 32 (c). Background wavenumbers shown in Figure 32 (a) were subtracted and further analysis of this spectrum is shown in Table 19, in order to accurately analyze which functional groups are present. The C=O carbonyl group peaks generally fall between from 1600 and 1900 cm^{-1}. The NO_2 nitro functional groups also fall between 1515 and 1560 cm^{-1}. So, the presence of either functional group was predicted from the FT-IR spectra analysis with a shift to 1573.71 cm^{-1} [51] [52]. The presence of Alkene and Alkyl halide groups was also detected as clearly shown in Table 19.

Table 19. Analysing FT-IR Spectrum of copper corroded sample in DPLE inhibited raw water

Sample Name	Wavenumber (cm^{-1})	Functional Group	Functional Group Formula	Wavenumber Range	Intensity
Corroded Cupper in DPLE Solution	1573.71	Carbonyl	C=O	1670-1820	Strong
	1573.71	Nitro	NO_2	1515-1560	Strong
	1117.17	Amine	C-N	1080-1360	Medium
	918.41	Alkene	C=C-H	675-1000	Strong
	870.73				
	830.26				
	785.98	Alkyl halide	C-Cl	600-800	Strong
	746.76				
	679.45				

Figure 32(b) shows the FT-IR spectrum analysis of the DPLE powder and Table 20 shows that spectrum analysis after subtracting the background wavenumbers, in order to accurately investigate the functional groups found in DPLE. The C=O carbonyl group peaks generally fall between from 1670 and 1820 cm^{-1} and was present at 1733.01 cm^{-1}. The NO_2 nitro functional groups also falls between 1515 and 1560 cm^{-1} and was present at 1515.43 and 1607.25 cm^{-1}. The presence of C=C aromtic ring and Alkyl halide groups was also detected as clearly shown in Table 20.

Table 20. Analysing FT-IR Spectrum of DPLE powder

Sample	**Wavenumber (cm^{-1})**	**Functional Group**	**Functional Group Formula**	**Wavenumber Range**	**Intensity**
DPLE Powder	1733.01	Carbonyl Compound	C=O	1670-1820	Strong
	1607.25	Nitro	NO_2	1515-1560 and 1345-1385	Strong
	1515.43				
	1461.62	Aromatic ring	C=C	1400-1600	Medium- Weak
	1444.82				
	1375.89				
	779.26	Alkyl halide	C-Cl	600-800	Strong
	718.86				
	667.44				
	631.23				
	596.39		C-Br	500-600	Strong
	588.57				
	570.35				
	564.39				
	557.81				

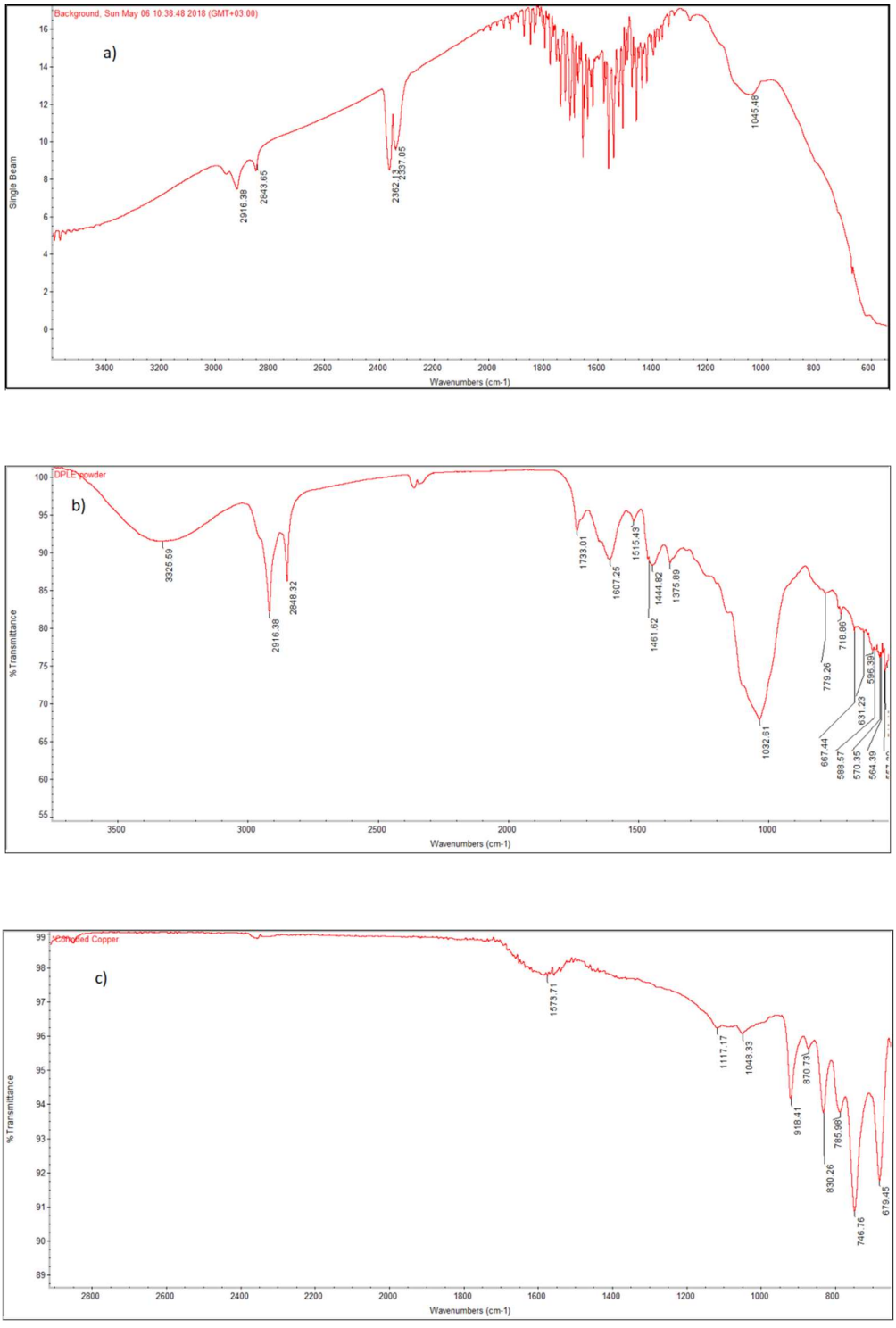

Figure 32. FT-IR spectrum results for a) background b) DPLE Powder c) corroded copper sample in DPLE inhibited raw water.

5.8 Surface Morphology

The SEM Spectroscopy images of the fresh copper sample specimen and specimen immersed in DPLE inhibited raw water are shown in Figures 33 (a) and (b). Compared to Figure 33(a), analysis of the image in Figure 33 (b) shows the presence of a layer, possibly resulting from a film of adsorbed functional groups from the DPLE solution on the copper metal surface.

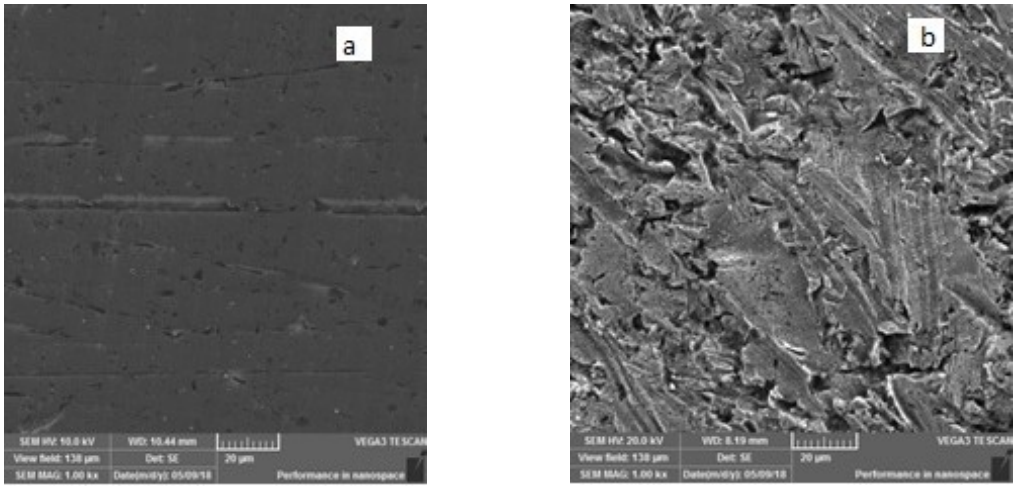

Figure 33. SEM Images of a) bare copper sample, and b) corroded copper sample in DPLE raw water solution.

5.9 Synergistic Effects

The DPLE was tested and found to have good inhibition efficiencies as a corrosion inhibitor of copper in raw water solutions. Sodium Tungstate (Na_2WO_4) and Potassium Iodide (KI) were selected to separately investigate its individual synergetic effect on the performance of DPLE in inhibiting copper corrosion in raw water solutions [44] [53].

Firstly, the results of synergism study of Sodium Tungstate are shown in Table 21. The inhibition efficiency of individual Sodium Tungstate (Na_2WO_4), DPLE, and their combination on copper was investigated using PDP. Figure 34 shows PDP curves with a clear shift in Tafel slop of DPLE and Na_2WO_4 combination towards higher current density values confirming lower inhibition than individual results. Hence, there was no beneficial synergy.

Table 21. Potentiodynamic polarization (PDP) results for Na_2WO_4 and DPLE synergized in raw water with copper specimen

Sample	**β_a** (V/decade)	**β_c** (V/decade)	**I_{corr}** (nA/cm^2)	**E_{corr}** (mV)	**Corrosion Rate** (mmy^{-1})	**Inhibition Efficiency** (%)
Blank	0.085	0.061	3511	-167	0.0308	-
DPLE 2000 ppm	0.028	0.029	147	-155	0.0013	96 %
Na_2WO_4 250 ppm	0.027	0.028	283	-106	0.0025	92%
DPLE 2000 ppm and Na_2WO_4 250 ppm	0.089	0.180	1008	-146	0.0089	71%

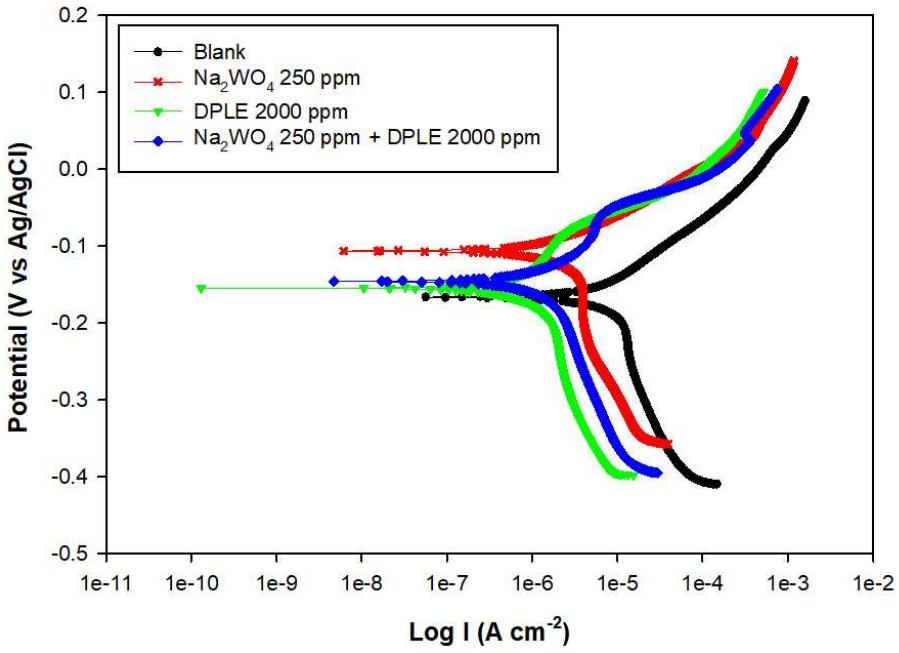

Figure 34. Potentiodynamic polarization (PDP) curves for the combination of 500 ppm and Na_2WO_4 250 ppm.

Secondly, the synergism parameters of Potassium Iodide are shown in Table 22. The inhibition efficiency of individual Potassium Iodide (KI), DPLE, and their synergistic combination on copper was investigated using PDP. The results showed that synergistic combination of Potassium Iodide (KI) and DPLE had 25% and 32% higher inhibition efficiency than individual results of 500 ppm of DPLE and 100 ppm KI, respectively. PDP results in Table 22 and PDP curves shown in Figures 35 and 36 also show a shift in Tafel slop of the combination of DPLE, with KI 100 and KI 50 ppm towards lower current density values confirming synergistic inhibition. However, when KI 25 ppm was added to DPLE, the shift was towards higher current density confirming there was no beneficial synergy at this concentration of KI.

Table 22. Potentiodynamic polarization (PDP) results for KI and DPLE synergized in raw water with copper specimen.

Sample	**β_a** (V/decade)	**β_c** (V/decade)	**I_{corr}** (nA/cm^2)	**E_{corr}** (mV)	**Corrosion Rate** (mmy^{-1})	**Inhibition Efficiency** (%)
Blank	0.085	0.061	3511	-167	0.0308	-
DPLE 500 ppm	0.070	0.127	1138	-68.1	0.0100	67%
KI 100 ppm	0.028	0.136	1274	-225	0.0112	64%
DPLE 500ppm & KI 100 ppm	0.037	0.129	583	-198	0.0048	84%
KI 50 ppm	0.020	0.155	2480	-171	0.0218	35%
DPLE 500 ppm & KI 50 ppm	0.044	0.059	460	-186	0.0040	87%
DPLE 500 ppm & KI 25 ppm	0.046	0.199	2660	-166	0.5219	57%

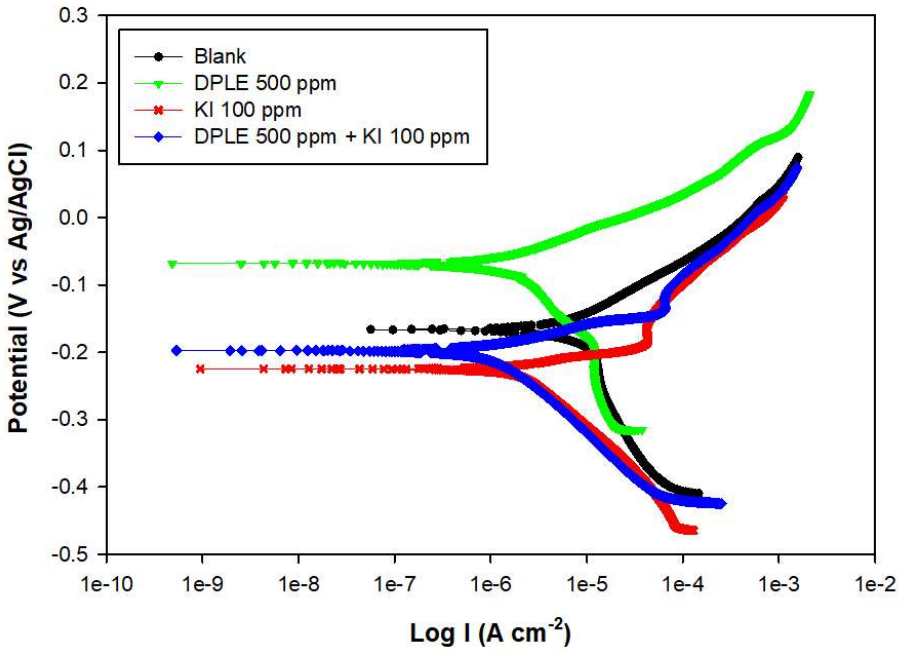

Figure 35. Potentiodynamic polarization (PDP) curves for synergistic combination of DPLE 500 ppm and KI 100 ppm.

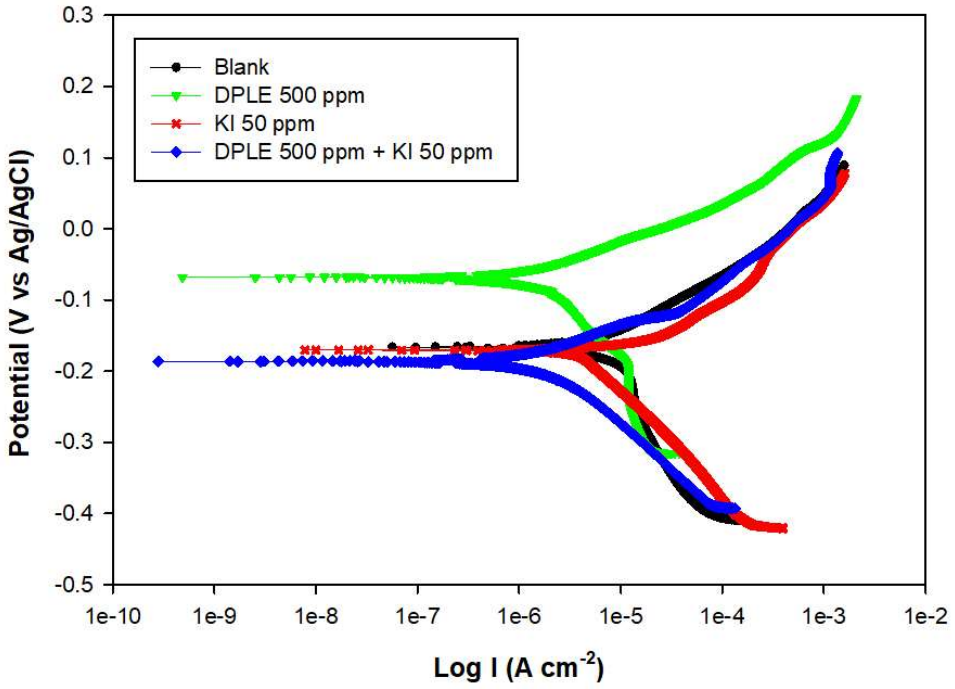

Figure 36. Potentiodynamic polarization (PDP) curves for synergistic combination of DPLE 500 ppm and KI 50 ppm.

It was observed from PDP results that the DPLE-KI combination exhibited higher inhibition efficiency than either DPLE or KI separately. As explained earlier, this could arise because of the co-adsorption of the iodide anions and cations from DPLE functional groups on the metal surface. However, co-adsorption could be competitive or cooperative [43]. In competitive co-adsorption, the anions and cations adsorb on different sites on the metal surface, whereas cooperative co-adsorption has to do with the adsorption of the cations on the anion layer [48]. Nevertheless, these two kinds of co-adsorption can take place simultaneously on the same metal surface. The synergism parameter (S_θ) is usually used to establish the kind of co-adsorption prevailing over the other on a metal surface. Generally, $S_\theta < 1$ is indicative of competitive co-adsorption and the existence of

antagonistic behavior, while $S_\theta > 1$ signifies the synergistic effect [43] [48]. The synergism parameter (S_θ) can be estimated by the following equation:

$$S_\theta = \frac{1-(\theta_1 + \theta_1 - \theta_1\theta_2)}{1 - \theta^{l}_{1+2}} \quad (16)$$

where θ_1 is the degree of surface coverage of DPLE, θ_2 is the degree of surface coverage of KI, and θ^{l}_{1+2} is the degree of surface coverage of the combination of DPLE and KI.

Table 23. Synergism parameters and co-adsorption types for DPLE with two different concentrations of KI using Potentiodynamic polarization (PDP) results.

Sample	**Inhibition Efficiency** (%)	**Surface Coverage** θ	**Synergism Parameter** S_θ	**Co-adsorption Type**
DPLE 500 ppm & KI 100 ppm	84%	0.84	0.8	competitive
DPLE 500 ppm & KI 50 ppm	87%	0.87	1.6	cooperative - synergistic effect
DPLE 500 ppm & KI 25 ppm	57%	0.57	0.5	competitive

It is obvious that the enhanced corrosion inhibition of DPLE by iodide ions was most probably due to competitive co-adsorption when KI concentrations of 100 was used, as the S_θ value was lower than unity. This can be explained by the increased concentration of iodide ions in the solution to near saturation levels when KI concentration was 100 ppm. The corrosion inhibition of DPLE increased when KI concentration was 50 ppm, which was due to a synergistic effect, as the S_θ value was greater than unity. The addition of KI 25 ppm to DPLE did not result in beneficial synergy.

Table 24. Corrosion rate calculated from weight-loss data of copper in raw water and inhibition efficiency as a function of inhibitor concentration in 112 h immersion at 22°C

Inhibitor Concentration (ppm)	**Initial Weight** (g)	**End Weight** (g)	**Lost Weight** (g)	**Corrosion Rate** (mmy^{-1})	**Inhibition Efficiency** (%)
Blank	20.6715	20.6704	0.0011	0.0327	-
DPLE 2000	20.7234	20.7231	0.0003	0.0081	75%
Na_2WO_4 250 ppm	22.7597	22.7595	0.0002	0.0054	84%
DPLE 2000 & Na_2WO_4 250 ppm	22.5389	22.5383	0.0006	0.0171	48%
DPLE 500 ppm	20.2226	20.2221	0.0005	0.0140	57%
KI 100 ppm	20.2231	20.2225	0.0006	0.0162	51%
DPLE 500 ppm & KI 100 ppm	23.1015	23.1012	0.0003	0.0083	74%
KI 50 ppm	20.7369	20.7361	0.0008	0.0228	30%
DPLE 500 ppm & KI 50 ppm	20.7349	20.7346	0.0003	0.0081	75%

Table 25. Synergism parameters and co-adsorption types for DPLE with two different concentrations of KI using weight loss results.

Sample	Inhibition Efficiency (%)	Surface Coverage θ	Synergism Parameter S_θ	Co-adsorption Type
DPLE 500 ppm & KI 100 ppm	74%	0.74	0.8	competitive
DPLE 500 ppm & KI 50 ppm	75%	0.75	1.2	cooperative - synergistic effect

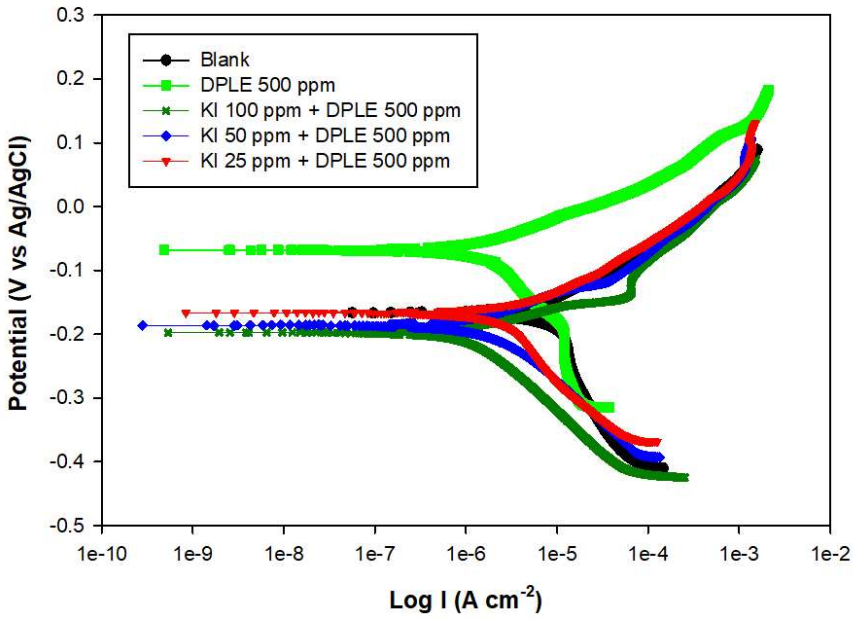

Figure 37. PDP curves for the corrosion of copper in raw water with a combination of DPLE and different concentrations of KI.

Table 25 shows the synergistic parameters and co-adsorption types for DPLE 500 ppm with KI 100 and 50 ppm concentrations using weight loss results. When KI concentration of 100 ppm was added to DPLE 500 ppm, the results showed that the enhanced corrosion

inhibition of DPLE by iodide ions was due to competitive co-adsorption, as the S_θ value was lower than unity. When KI concentration of 50 ppm was added to DPLE 500 ppm, the results showed that the enhanced corrosion inhibition of DPLE by iodide ions was due to synergistic effect and cooperative co-adsorption, as the S_θ value was lower than unity [54].

Figure 37 shows Tafel curves for the combination of DPLE 500 ppm with KI 100 and 50 ppm shifted towards lower current densities than DPLE and KI alone, while the Tafel curve for the combination of KI 25 ppm and DPLE 500 ppm shifted towards a higher current density.

Synergism parameters obtained from both PDP and weight loss (Tables 23 and 25, respectively) showed the same co-adsorption types when weight loss data was used.

6 CONCLUSIONS

- DPLE acts as an inhibitor for copper corrosion in raw water. The inhibition effect is concentration-dependent.
- The results of PDP measurements indicated that organic BBMHB behaved as a mixed inhibitor while green DPLE acted as a cathodic inhibitor.
- The results obtained from all three methods (i.e. weight loss, PDP and EIS) converged and supported the effectiveness of DPLE as an inhibitor of copper corrosion in raw water.
- The optimum concentration of green DPLE corrosion inhibitor is 2000 ppm for mitigating copper corrosion in raw water.
- Increasing the temperature of raw water decreased the inhibition efficiency of DPLE for copper corrosion.
- Increasing the immersion time of copper in raw water increased the inhibition efficiency of DPLE.
- Both green DPLE and organic BBMHB corrosion inhibitors followed the Langmuir adsorption isotherm.
- The combination of DPLE and Sodium Tungstate (Na_2WO_4) did not have beneficial synergy for inhibiting copper corrosion in raw water.
- The combination of DPLE and Potassium Iodide (KI) with 100 and 50 ppm showed strong synergistic effect on copper corrosion in raw water.

7 REFERENCES

[1] E. McCafferty, Introduction to Corrosion Science, Alexandria, VA: Springer, 2009.

[2] R. W. Revie and H. H. Uhlig, Corrosion and Corrosion Control, An Introduction to Corrosion Science and Engineering, 4th ed., Hoboken, NJ: A John Wiley & Sons, Inc., 2008.

[3] C. Wagner, W. Traud, "On the Interpretation of Corrosion Processes Through the Superposition of Electrochemical Partial Processes and on the Potential of Mixed Electrodes," *Corrosion ,* vol. 62, no. 10, pp. 844 -855, 2006.

[4] M. Schock, "Internal corrosion and deposition control" in Water Quality and Treatment: A Handbook of Community Water Supplies, New York, NY: McGraw-Hill Inc., 1999.

[5] S. Bradford, Corrosion Control, New York: Van Nostrand Reinhold, 1993, p. 354.

[6] F. W. Pontius, "Lead and copper rule revisions proposed," *American Water Works Association Journal,* vol. 88, no. 16, 1996.

[7] D.A. Lytle, M.R. Schock, "Pitting corrosion of copper in waters with high pH and low alkalinity," *American Water Works Association Journal,* vol. 100, no. 14, pp. 115-129, 2008.

[8] J. F. Bosich, Corrosion Prevention for practicing Engineers, New York: Bames and Noble, 1970.

[9] L. V. F, "Mechanism of pitting corrosion of copper in supply waters," *British Corrosion Journal,* no. 2, p. 175, 1967.

[10] H. Campbell, "Pitting Corrosion in copper water pipes caused by films of carbonaceous material produced during manufacture," *Journal Inst Metals,* no. 345.

[11] L. Kenworthy, "The problem of copper and galvanized iron in the same water system," *Journal Inst Metals ,* no. 69, pp. 67-90, 1943.

[12] P.J. Bremer , B.J. Webster , D. Brettkelly, "Biocorrosion of copper in potable water," *American Water Works Association Journal,* vol. 93, no. 8, pp. 82-91, 1993.

[13] M.F. Obrecht; L.L. Quill, "How Temperature, Treatment, and Velocity of Potable Water Affect Corrosion of Copper and its Alloys in heat exchanger and piping systems," *Heating, Piping and Air Conditioning,* vol. 32, no. 5, pp. 105-169, 1960.

[14] I. Singh and D.S. Mavinic, "Significance of building and plumbing specifications on trace metal concentrations in drinking water," *Canadian Journal of Civil Engineering,* vol. 18, pp. 893-903, 1991.

[15] D.M. Macquarrie , D.S. Mavinic , D.G. Neden, "Greater Vancouver Water District drinking water corrosion inhibitor testing," *Canadian Journal of Civil Engineering,* vol. 24, no. 1, pp. 34-52, 1997.

[16] M. Edwards, J. F. Ferguson, "Accelerated testing of copper corrosion.," *American Water Works Association Journal,* vol. 85, no. 10, pp. 105-113, 1993.

[17] M. Edwards and S. Jacobs, "The blue water phenomenon," *American Water Works Association Journal,* vol. 92, no. 7, pp. 72-82, 2000.

[18] R. Droste, Theory and Practice of Water and Wastewater Treatment, New York: John Wiley & Sons, Inc., 1997.

[19] D. Atlas , J. Coombs and O. T. Zajicek, "The corrosion of copper by chlorinated drinking waters," *Water Res. ,* vol. 16, pp. 693-698, 1982.

[20] A. Stone, D. Spyridakis, M. Benjamin, J. Ferguson, S. Reiber and S. Osterhus, "The effects of short-term changes in water quality on copper and zinc corrosion rates," *American Water Works Association Journal,* vol. 79, no. 2, pp. 75-82, 1987.

[21] A.K. Singh, M.A. Quraishi, "The effect of some bis-thiadiazole derivatives on the corrosion of mild steel in hydrochloric acid," *Corros. Sci.,* no. 52, p. 1373–1385, 2010.

[22] M.A. Amin, K.F. Khaled, "Copper corrosion inhibition in O2-saturated H2SO4 solutions," *Corros. Sci.,* vol. 52, no. 4, p. 1194–1204, 2010.

[23] D. Bancroft, "Corrosion Control Program in Denvers," *Massachusetts Journal. NEWWA,* vol. 102, no. 3, p. 163, 1988.

[24] B.P. Boffardi and A.M. Sherbondy, "Control of lead Corrosion by Chemical Treatment," *Corrosion Engineering,* vol. 47, no. 12, pp. 966-975, 1991.

[25] M. Edwards, L. Hidmi, D. Gladwell, "Phosphate inhibition of soluble copper corrosion by product release," *Corrosion science,* vol. 44, no. 5, pp. 1057-1071, 2002.

[26] L.R. Chauhan, G. Gunasekaran, "Corrosion inhibition of mild steel by plant extract in dilute HCl medium," *Corrosion Science,* vol. 49, no. 3, pp. 1143-1161, 2007.

[27] B.A. Abd-El-Nabey, A.M. Abdel-Gaber, E. Khamis,S. El-Housseiny, M.E. Ali, "Inhibitive Action of Cannabis Plant Extract on the Corrosion of Copper in 0.5 M H2SO4," *Int. J. Electrochem Sci.,* vol. 8, no. 5, pp. 7124-7137, 2013.

[28] A.M. Abdel-Gaber, B.A. Abd-El-Nabey, I.M. Sidahmed, A.M. El-Zayady, M. Saadawy, "Inhibitive action of some plant extracts on the corrosion of steel in acidic media," *Corrosion Science,* vol. 48, pp. 2765-2779, 2006.

[29] K.O. Orubite, N.C. Oforka, "Inhibition of the corrosion of mild steel in hydrochloric acid solutions by the extracts of leaves of Nypa fruticans Wurmb," *Materials Letters,* vol. 58, pp. 1768-1772, 2004.

[30] L. Valek, S. Martinez, "Copper corrosion inhibition by Azadirachta indica leaves extract in 0.5 M sulphuric acid," *Materials Letters,* vol. 61, pp. 148-151, 2007.

[31] P.C. Okafor, E.E. Ebenso, U.J. Ekbe, "Azadirachta indica extracts as corrosion inhibitor for mild steel in acidic medium," *Int. J. Electrochem. Sci,* vol. 5, no. 7, p. 978–993, 2010.

[32] M. Dayeb, "Egyptian licorice extract as a green corrosion inhibitor for copper in hydrochloric acid solution," *J of Ind & Eng Chem,* vol. 22, pp. 384-389, 2015.

[33] S.A. Umoren, Z.M. Gasem, I.B. Obot, "Natural Products for Material Protection: Inhibition of Mild Steel Corrosion by Date Palm Seed Extracts in Acidic Media," *I & EC,* vol. 52, pp. 14855-14865, 2013.

[34] S.A. Umoren, Z.M. Gasem, I.B. Obot, "Date palm (Phoenix dactylifera) leaf extract as an eco-friendly corrosion inhibitor for carbon steel in 1M hydrochloric acid solution," *Anti-Corrosion Methods & Materials,* vol. 62, no. 1, pp. 19-28, 2015.

[35] Da-quan Zhang, Li-xin Gao, Guo-ding Zhou, "Inhibition of copper corrosion in aerated hydrochloric acid solution by heterocyclic compounds containing a mercapto group," *Corrosion Science,* vol. 46, no. 12, pp. 3031-3040, 2004.

[36] P. Kalaiselvi , S. Chellammal, S. Palanichamy, G. Subramanian, "Artemisia pallens as corrosion inhibitor for mild steel in HCl medium," *Materials Chemistry and Physics,* vol. 120, p. 643–648, 2010.

[37] K. Krishnaveni . J. Ravichandran, "A Study on the Inhibition of Copper Corrosion in Sulphuric Acid by Aqueous Extract of Leaves of Morinda tinctoria," *J Fail. Anal. and Preven.,* vol. 15, p. 711–721, 2015.

[38] A.M. Shah, A.A. Rahim, S.A. Hamid, S. Yahya, "Green inhibitors for copper corrosion by mangrove tannin," *Int. J. Electrochem.Sci.,* vol. 8, p. 2140–2153, 2013.

[39] R. Senthooran, N. Priyantha, "Inhibition of corrosion of copper in HCl by Tea Leaves Extracts: I. Corrosion rate measurements.," *Annual Research Journal of SLSAJ,* vol. 12, p. 1–10, 2012.

[40] P.C. Okafor, E.A. Apebende, "Corrosion inhibition characteristics of Thymus vulgaris, Xylopia aethiopica and Zingiber officinale extracts on mild steel in H2SO4 solutions," *Pigment & Resin Technology,* vol. 43, no. 6, pp. 357-364, 2014.

[41] M.E. Al-Dokheily, H.M. Kredy, R.N. Al-Jabery, "Inhibition of Copper Corrosion in H2SO4, NaCl and NaOH Solutions by Citrullus colocynthis Fruits Extract," *Journal of Natural Sciences Research,* vol. 4, no. 17, pp. 60-73, 2014.

[42] E.-S. M. Sherif, "Effects of 2-amino-5-(ethylthio)-1,3,4-thiadiazole on copper corrosion as a corrosion inhibitor in 3% NaCl solutions," *Applied Surface Science,* vol. 252, p. 8615–8623, 2006.

[43] A.A. Farag, T.A. Ali, "The enhancing of 2-pyrazinecarboxamideinhibition effect on the acid corrosion of carbon steel in presence of iodide ions," *J of Ind Eng Chem,* vol. 21, p. 627–634, 2015.

[44] V.S. Saji, S.M.A. Shibli, "Synergistic inhibition of carbon steel corrosion by sodium tungstate and sodium silicate in neutral aqueous media," *Anti-Corrosion Methods and Materials,* vol. 49, no. 6, pp. 433-443, 2002.

[45] M.M. Solomon, S.A. Umoren, A.U. Israel, I.G. Etim, "Synergistic inhibition of aluminium corrosion in H2SO4 solution by polypropylene glycol in the presence of iodide ions," *Pigm Resin Technol,* vol. 45, no. 4, p. 280–293, 2016.

[46] Haroon A. M. Saeed, Yu Liu, Lucian A. Lucia, Honglei Chen, "Sudanese Agro-residue as a Novel Furnish for Pulp and Paper Manufacturing," *BioResources,* vol. 12, no. 2, pp. 4166-4176, 2017.

[47] W. Liu, A. Singh, Y. Lin, E.E. Ebenso, L. Zhou, B. Huang, "8-Hydroxyquinoline as an effective corrosion inhibitor for 7075 aluminium alloy in 3.5% NaCl solution," *Int J Electrochem Sci,* vol. 9, pp. 5574-5584, 2014.

[48] P. Muorya, P. Singh, R.B. Rastogi, M.M. Singh, "Inhibition of mild steel corrosion by 1,4,6-trimethyl-2-oxo-1,2-dihydropyridine-3-carbonitrile and synergistic effect of halide ion in 0.5 M H2SO4.," *Appl Surf Sci,* vol. 380, pp. 141-150, 2016.

[49] Z. Tao, W. He, S. Wang, S. Zhang, G. Zhou, "A study of differential polarization curves and thermodynamic propertiesfor mild steel in acidic solution with nitrophenyltriazole derivative.," *Corrosion Science,* vol. 60, pp. 205-213, 2012.

[50] M.M. Solomon, S.A. Umoren, I.I. Udousoro, A.P. Udoh, "Inhibitive and adsorption behavior of carboxymethyl cellulose on mild steel corrosion in sulphuric acid solution," *Corrosion Science,* vol. 52, p. 1317–1325, 2010.

[51] S. Pongpiachan, "FTIR Spectra of Organic Functional Group Compositions in PM2.5 Collected at Chiang-Mai City Thailand during the Haze Episode in March 2012," *Journal of Applied Sciences,* vol. 14, pp. 2967-2977, 2014.

[52] R.M. Silverstein, G.C. Bassler and T.C. Morrill, Spectrometric Identification of Organic Compounds, New York, USA: John Wiley and Sons, 1981.

[53] Y. C. Wu, P. Zhang, H. W. Pickering, D. L. Allara, "Effect of KI on Improving Copper Corrosion Inhibition Efficiency of Benzotriazole in Sulfuric Acid Electrolytes," *J. Electrochem. Soc.,* vol. 140, no. 10, pp. 2791-2800, 1993.

[54] M. M. Solomon, Husnu Gerengi, Tugce Kaya, Ertuğrul Kaya & S. A. Umoren, "Synergistic inhibition of St37 steel corrosion in 15% H2SO4 solution by chitosan and iodide ion additives," *Cellulose,* vol. 24, p. 931–950, 2017.

Vitae

Name	: Abdul-Rahman A.H. Nour
Nationality	: Canadian
Date of Birth	:5/10/1971
Email	: ar.nour@yahoo.com
Address	: Windsor, Ontario, Canada
Academic Background	: Bachelor of Science in Mechanical Engineering (1993) Jordan University of Science and Technology, Irbid, Jordan
Professional Background	: A Mechanical Engineer with over 24 years of experience in the areas of:

- Corporate Management, Strategic Planning & Risk Evaluation
- Project Management, Scheduling, Planning and Cost Control.
- Caterpillar Service Management, Control and Logistics.
- Caterpillar Rental Fleet and Organizational Management.